Previous studies have reported that PU.1 is also down-regulated in cHL cells via methylation of the *PU.1* promoter.[23] Therefore, in this study, we evaluated whether PU.1 is tumor suppressor in cHL cells.

Methods

Bisulfite sequencing

Genomic DNA was treated with sodium bisulfite as previously described[20] and subjected to 35 cycles of PCR. A 149-bp *PU.1* promoter-exon1 region, including a PU.1 binding site, was amplified with the primers 5′-GTAGTTTAGGGGGTAGGTTTGAGTT-3′and 5′-AAAAAAAACCC-TTCCATTTTACAC-3′. PCR products were directly sequenced. A 244-bp product encompassing the −17 kb URE, including PU.1 and runt-related transcription factor 1 (RUNX1/AML1) binding sites, which are required for PU.1 expression, was amplified with the primers 5′-ATTTTTTT-GAGGTTTGGTTTAGGTT-3′ and 5′-CTACAACTACCCCTATTTCC-ACATC-3′. Both regions were previously shown to contain CpG islands.[20]

Cell culture

Human Hodgkin lymphoma cell lines L428, KM-H2, L540, HDLM2, and HD-70 and their derivatives were grown in RPMI 1640 medium containing 10% (volume/volume) FBS at 37°C.

Constructs

pCAG20-1, pUHD-3 puromycin and pUHD-10-3 IRES-GFP plasmids were kind gifts from Dr Takumi Era (Division of Molecular Neurobiology, Institute of Molecular Embryology and Genetics, Kumamoto University, Japan).[24] The human PU.1 cDNA was subcloned into the blunt-ended *EcoR*I site of pUHD10-3 IRES-GFP, resulting in pUHD10-3 PU.1-IRES-GFP.

Generation of stable transformants conditionally expressing PU.1

To obtain PU.1-inducible cHL cell lines using the tetracycline-off system, 1×10^7 L428 or KM-H2 cells were cotransfected with 10 μg each of *Sca*I-digested pCAG20-1 and pUHD-3 puromycin plasmids by electroporation. Cells were selected with 1 μg/mL puromycin, and subsequently transfected with 10 μg of *Sca*I-digested pUHD10-3 PU.1-IRES-GFP and 2 μg of *Hin*dIII-digested pPGKneo.[20] After isolation of G418-resistant clones, GFP expression was evaluated after tetracycline removal. On confirmation of GFP expression, these cells were designated L428$^{tetPU.1}$ and KM-H2$^{tetPU.1}$.

Xenograft model

A total of 7×10^6 L428$^{tetPU.1}$ or KM-H2$^{tetPU.1}$ cells were injected subcutaneously into *Rag2*$^{-/-}$*Jak3*$^{-/-}$ *balb/c* mice (n = 16 per group). Mice were given drinking water containing tetracycline (500 μg/mL) 3 days before injection. Subcutaneous tumors were grown to 1- to 2-cm in diameter (~ 30-35 days after injection), and half of the cohort (n = 8) were maintained on tetracycline-treated water, whereas the remaining mice discontinued tetracycline and were given pure water. Tumor size was measured every 7 days.

Primary cHL cells

Primary cells were obtained from lymph node biopsy samples of 3 patients with cHL. Informed consent for sample collection was obtained according to protocols approved by the institutional review boards and in accordance with the Declaration of Helsinki. Primary cHL cells were purified by negative selection using an anti-CD3, CD14, CD16, CD19, CD20, and CD56 antibody cocktail (BioLegend) and antimouse IgG antibody-conjugated magnetic beads (Miltenyi Biotec). After negative selection, the purity of Hodgkin cells was confirmed by May-Giemsa staining and immunostaining with anti-CD30 antibody of cytospin samples or flow cytometry after staining with anti-CD30 antibody.

Lentiviral transduction

The CSII-EF-MCS-IRES-Venus lentiviral vector and packaging constructs, VSV-G Rev and CAG-HIVgp, were purchased from the RIKEN Bio Resource Center. The human PU.1 cDNA was subcloned into *Not*I site of CSII-EF-MCS-IRES-Venus. Virus was produced and cells were infected as previously described (http://www.brc.riken.jp/lab/cfm/Subteam_for_Manipulation_of_Cell_Fate/Home.html).[25,26]

DNA microarray analysis

Total RNA was extracted from L428$^{tetPU.1}$ and KM-H2$^{tetPU.1}$ cells using Trizol reagent at 3 different time points: days 0, 1, and 3 after tetracycline removal. RNA was hybridized to Illumina:Sentrix Human-6 Expression BeadChips or Illumina HumanHT-12 Version 4 Expression BeadChips, according to the manufacturer's instructions. Gene expression profiles were analyzed using GeneSpring Version 12.0 software.[27] Data for L428$^{tetPU.1}$ cells are available at the Gene Expression Omnibus under accession number GSE42437; data for KM-H2$^{tetPU.1}$ cells are available under GSE42440.

Real-time PCR

Quantitative TaqMan PCR was performed with commercially available assay-on demand probe primer sets for *p21* and *β-actin* (Applied Biosystems) and TaqMan Universal PCR Master Mix reagent according to the manufacturer's instructions. Reactions were performed using an Illumina Eco Real-Time PCR system. The expression levels of *β-actin* were used to normalize the relative expression levels of *p21*. The expression level of *p21* in L428$^{tetPU.1}$ cells before tetracycline removal was set to 100.

Western blot analysis

Cell lysates were resolved by SDS-PAGE and transferred onto nitrocellulose membranes. The membranes were incubated with anti-PU.1, anti-p21$^{WAF/CIP1}$, and antiactin primary antibodies (Santa Cruz Biotechnology) for 3-12 hours. Membranes were then incubated with peroxidase-labeled secondary antibodies for 30 minutes and developed using an enhanced chemiluminescence system (GE Healthcare).

Generation of L428$^{tetPU.1}$ cells stably expressing p21 siRNA

siRNA expression vectors were generated by insertion of annealed oligonucleotides targeting p21 and scrambled control siRNAs into the *BamH*I and *Hin*dIII sites of pRNA-U6.1/Zeo or pRNA-U6.1/ Hygro (GenScript).[27] siRNA expression vectors were transfected into L428$^{tetPU.1}$ cells by electroporation, and stable transformants were obtained by selection with zeocin (400 μg/mL) or hygromycin (200 μg/mL).

Detection of apoptosis

For detection of apoptosis, cHL cells were stained with an annexin V Phycoerythrin or Allophycocyanin Apoptosis Detection kit (Medical and Biologic Laboratories). Cells were analyzed using a FACSCalibur flow cytometer (Becton Dickinson).

Cell-cycle analysis

L428$^{tetPU.1}$ and KM-H2$^{tetPU.1}$ cell-cycle profiles were analyzed by staining with bromodeoxyuridine (BrdU) and 7-aminoactinomycin D (BrdU Flow Kits; BD Biosciences PharMingen),[28] 3 days after tetracycline withdrawal. Cells were analyzed by flow cytometry (FACSCalibur).

Results

PU.1 is down-regulated in Hodgkin lymphoma by methylation of the promoter and a −17 kb URE of the PU.1 gene

Previous studies have shown that PU.1 is generally highly down-regulated in both Hodgkin lymphoma cell lines and primary Hodgkin lymphoma cells.[23] In these studies, methylation-specific PCR revealed that the *PU.1* promoter is methylated, leading to

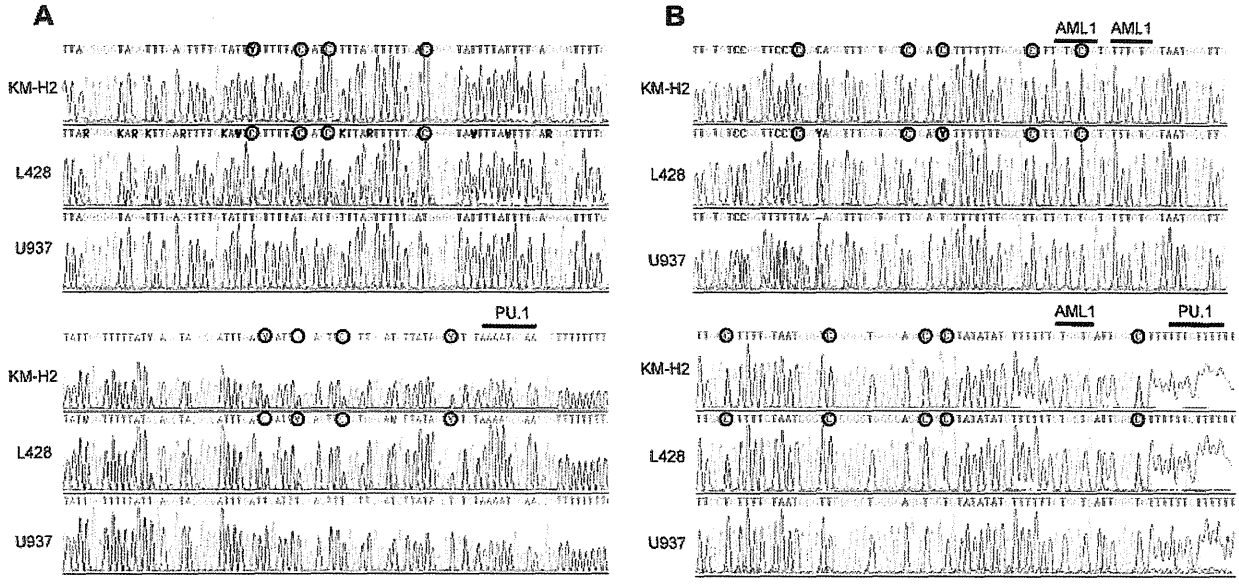

Figure 1. The promoter region and the −17 kb URE of the *PU.1* gene are highly methylated in cHL cells. (A) Bisulfite sequencing confirmed that the promoter of *PU.1* is highly methylated in L428 and KM-H2 Hodgkin lymphoma cell lines. ○ represents methylated cytosines. Underlining indicates the PU.1 binding site downstream of the translation initiation site. (B) Bisulfite sequencing revealed that the −17 kb URE was highly methylated in L428 and KM-H2 Hodgkin lymphoma cell lines. ○ represents methylated cytosines. Underlining indicates 3 RUNX1 (AML1) binding sites and a PU.1 binding site.

down-regulation of PU.1 expression. We previously demonstrated that PU.1 is strongly down-regulated in myeloma cell lines and the *PU.1* promoter was highly methylated as shown by bisulfite sequencing.[20] To confirm this mechanism of PU.1 down-regulation in Hodgkin lymphoma, we conducted bisulfite sequencing of the *PU.1* promoter region in the Hodgkin lymphoma cell lines, L428 and KM-H2. As shown in Figure 1A, the *PU.1* promoter region was heavily methylated in both cell lines, and there was no C-T conversion in CpG islands after bisulfite treatment of genomic DNA. Gene expression often requires *cis*-elements located > 10 kb or, in some cases, more than several hundred kilobases upstream of the transcriptional start site or downstream of the transcriptional termination site.[29-36] The expression of PU.1 also requires a URE located −14 kb and −17 kb upstream of its promoter in mice and humans, respectively.[18,19,21,22] Previously, we reported that PU.1 is down-regulated in multiple myeloma cells via methylation of its promoter and the −17 kb URE.[20] We therefore evaluated the methylation status of the −17 kb URE of *PU.1* in L428 and KM-H2 cells. The −17 kb URE of *PU.1* was highly methylated in both L428 and KM-H2 cells, indicating that PU.1 is silenced in cHL cells via methylation of both the promoter and the −17 kb URE (Figure 1B).

PU.1 induces growth arrest and apoptosis of Hodgkin lymphoma cell lines, L428 and KM-H2

We next evaluated whether down-regulation of PU.1 may play a role in Hodgkin lymphoma cell growth. We generated Hodgkin lymphoma cell lines that conditionally express PU.1 using a tet-off system, designated L428$^{tetPU.1}$ and KM-H2$^{tetPU.1}$. After the removal of tetracycline from growth medium, PU.1 was highly up-regulated in both L428$^{tetPU.1}$ and KM-H2$^{tetPU.1}$ cell lines (Figure 2A). Conditional expression of PU.1 induced complete growth arrest of both L428$^{tetPU.1}$ and KM-H2$^{tetPU.1}$ cells over the course of 7 days (Figure 2B-C). Cell-cycle analysis using BrdU and 7-aminoactinomycin D staining revealed that induction of PU.1 led to a decrease in S phase cells in both L428$^{tetPU.1}$ (15.8% vs 1.4%) and KM-H2$^{tetPU.1}$ cells (32.1% vs 9.9%) after 3 days, suggesting that PU.1 induced G_1 arrest in these cells (Figure 2D). We also observed an increase in the sub-G_1 population in both L428$^{tetPU.1}$ and KM-H2$^{tetPU.1}$ cells. Consistent with these data, annexin V staining revealed that PU.1 expression led to a significant increase in apoptotic cells in L428$^{tetPU.1}$ and KM-H2$^{tetPU.1}$ cells at day 3 (28.5% vs 72.9% and 17.1% vs 81.7%, respectively; Figure 2E). Morphologically, L428$^{tetPU.1}$ cells expressing PU.1 were enlarged and displayed numerous cell processes and vacuoles of various sizes, which in some cases occupied the majority of the cellular mass and nuclear compartment (Figure 2F). In addition, a number of L428$^{tetPU.1}$ PU.1-expressing cells exhibited nuclear fragmentation, a typical feature of apoptosis (Figure 2F). In comparison, KM-H2$^{tetPU.1}$ cells expressing PU.1 contained relatively smaller vacuoles, and many cells exhibited nuclear condensation, which is also a feature of apoptotic cells. These data demonstrate that PU.1 induces complete growth arrest and apoptosis in L428 and KM-H2 cells.

PU.1 induces growth arrest, regression of subcutaneous tumors, and prolonged survival in a Hodgkin lymphoma xenograft mouse model

We next investigated the role of PU.1 in a xenograft model of Hodgkin lymphoma. A total of 7×10^6 L428$^{tetPU.1}$ or KM-H2$^{tetPU.1}$ cells were injected subcutaneously in *Rag2*$^{-/-}$*Jak3*$^{-/-}$ *balb/c* mice, and tumors were grown to 1- to 2-cm in diameter. Mice were then divided into 2 treatment groups: one group continued drinking tetracycline-treated water (n = 8), whereas the other group was given nontreated water (n = 8). In mice taking tetracycline, tumors continued to grow and increase in size (Figure 3A-B), and a number of mice developed skin ulcers possibly induced by tumor necrosis. In contrast, tumors in mice given nontreated water ceased to grow and decreased in size in several cases (Figure 3C-D). All mice injected with L428$^{tetPU.1}$ or KM-H2$^{tetPU.1}$ cells, taking tetracycline, died within 96 days or 143 days, respectively. In contrast, more than 50% of mice without tetracycline survived > 200 days in both xenograft models. Furthermore, mice given nontreated water and harboring tumors < 1 cm in diameter had a 100%

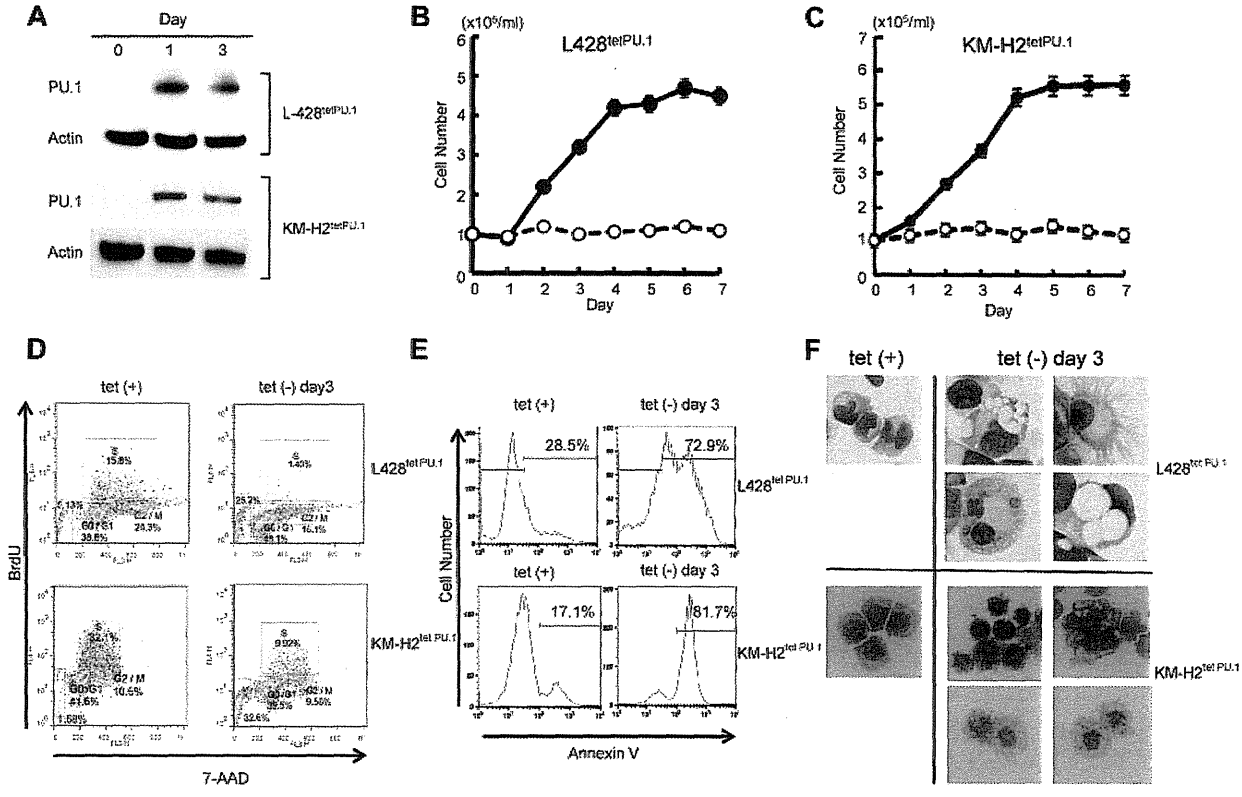

Figure 2. PU.1 induces growth arrest and apoptosis in L428 and KM-H2 cHL cell lines in vitro. (A) Western blot of PU.1 protein after tetracycline withdrawal. PU.1 was highly induced after tetracycline withdrawal in L428$^{tetPU.1}$ and KM-H2$^{tetPU.1}$ cells. PU.1 induced growth arrest in L428$^{tetPU.1}$ (B) and KM-H2$^{tetPU.1}$ cells (C) after tetracycline removal (○), whereas uninduced cells (●) grew comparably to wild-type parental cells. (D) Cell-cycle analysis was performed in L428$^{tetPU.1}$ and KM-H2$^{tetPU.1}$ cells by BrdU and 7-aminoactinomycin D staining. PU.1 induced G_1 arrest and led to a significant decrease in S-phase cells in L428$^{tetPU.1}$ and KM-H2$^{tetPU.1}$ cell lines. (E) PU.1 induced apoptosis in L428$^{tetPU.1}$ and KM-H2$^{tetPU.1}$ cells as assessed by annexin V staining. (F) PU.1 induced morphologic changes in L428$^{tetPU.1}$ and KM-H2$^{tetPU.1}$ cells. L428$^{tetPU.1}$ cells expressing PU.1 exhibited numerous different-sized cell processes and vacuoles compared with uninduced cells. A number of cells displayed nuclear fragmentation (Tet$^-$, day 3, bottom left panel). The majority of KM-H2$^{tetPU.1}$ cells expressing PU.1 also contained relatively small-sized vacuoles and nuclear condensation, indicative of apoptosis. Images were acquired using a BX60 microscope and DP70 digital camera with DP controller software (Olympus; ×400 magnification).

survival rate. In comparison, mice without tetracycline and harboring larger tumors tended to have skin ulcers at the site of the shrinking tumor and acquired lethal infections.

These data suggest that PU.1 may act as a tumor suppressor of cHL in vivo.

PU.1 induces apoptosis in primary cells purified from patients with Hodgkin lymphoma

Next, to evaluate whether PU.1 induces apoptosis of primary cHL cells, we purified lymphoma cells from the lymph nodes of patients with cHL. Negative selection was performed with anti-CD3, -CD14, -CD16, -CD19, -CD20, and -CD56 antibodies, and purified cells consisted of > 90% Hodgkin and Reed Sternberg-cells as confirmed by May-Giemsa staining of cytospin samples (Figure 4A). These cells were also CD30-positive as confirmed by flow cytometry or immunohistochemistry (supplemental Figure 1A-B, available on the *Blood* Web site; see the Supplemental Materials link at the top of the online article). After purification, primary Hodgkin lymphoma cells cultured alone survived for 1 day. However, coculture with cells obtained from patient lymph nodes prolonged survival to at least 3 days, as confirmed by microscopy of cytospin samples. Therefore, we infected cells obtained from whole lymph nodes, including Hodgkin cells, with lentivirus overexpressing human PU.1 or empty vector control. After 3 days in culture, primary Hodgkin lymphoma cells were purified by negative selection and subjected to annexin V staining. Cells transduced with lentivirus were recognized as Venus-positive cells and were analyzed by staining with propidium iodide (PI) and annexin V antibody. In case 1, overexpression of PU.1 led to a decrease in live cells (PI$^-$/annexin V$^-$) compared with empty vector (52.4% vs 69.8%), and a concomitant increase in PI$^-$/annexin V$^+$ preapoptotic cells (19.7% vs 8.6%; Figure 4B, left panel). In addition, primary cHL cells transduced with PU.1 exhibited various-sized vacuoles in cytosol (Figure 4A, right panels). In case 2, overexpression of PU.1 also led to a decrease in live cells (PI$^-$/annexin V$^-$) compared with control vector (9.4% vs 18.1%), and an increase in PI$^+$ apoptotic cells (PI$^+$/annexin V$^-$ and PI$^+$/annexin V$^+$) compared with vector only (81% vs 68%; Figure 4B, middle panel). In case 3, overexpression of PU.1 also led to a decrease in live cells (PI$^-$) compared with control vector (62.7% vs 92.1%) and an increase in PI$^+$ apoptotic cells (PI$^+$/annexin V$^-$ and PI$^+$/annexin V$^+$) compared with vector only (37.2% vs 17.9%; Figure 4B right panel). These experiments were performed in biologic duplicate with similar results. These data suggest that PU.1 also induces apoptosis in primary Hodgkin lymphoma cells.

Growth arrest of L428$^{tetPU.1}$ cells induced by PU.1 is at least partially dependent on up-regulation of p21

To elucidate the mechanisms underlying cell-cycle arrest and apoptosis induced by PU.1, we compared gene expression profiles

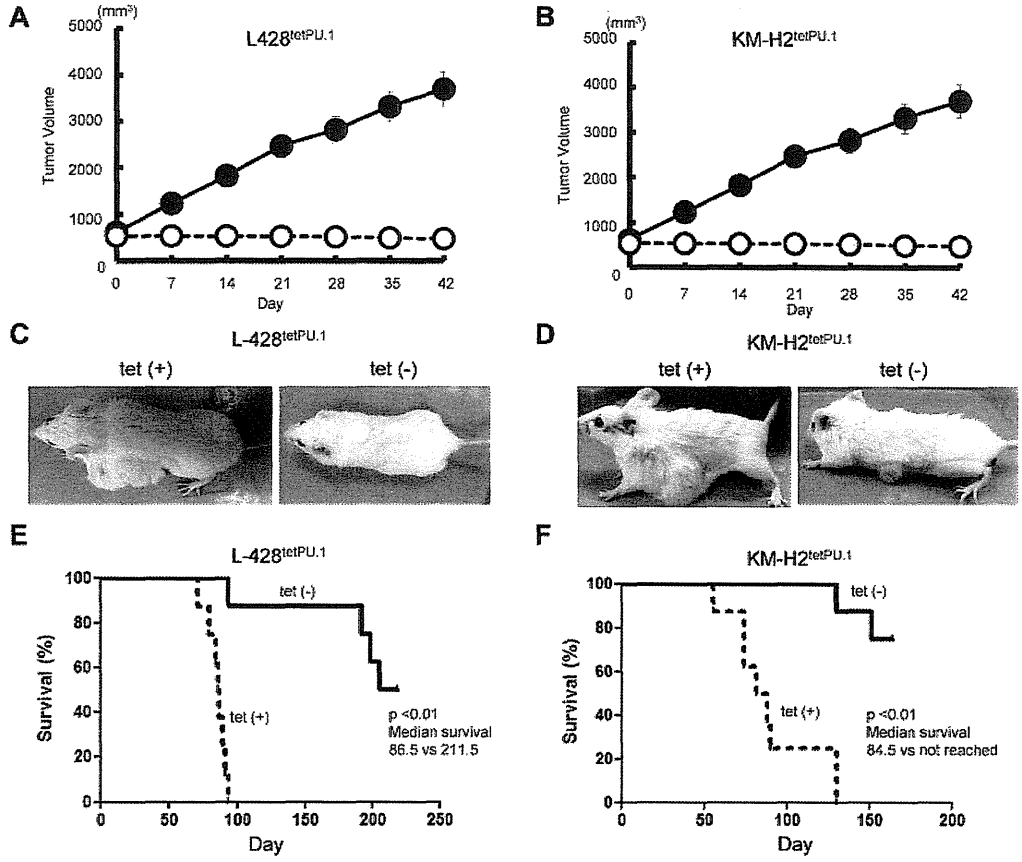

Figure 3. PU.1 induces growth arrest and apoptosis in both L428$^{tetPU.1}$ and KM-H2$^{tetPU.1}$ cHL cell lines in vivo. Tumor size in L428$^{tetPU.1}$ (A) and KM-H2$^{tetPU.1}$ (B) xenograft mouse models over the course of 7 days. Tumors in L428$^{tetPU.1}$ and KM-H2$^{tetPU.1}$ mice given tetracycline continued to grow (●), compared with tumors in mice without tetracycline, which ceased to grow and in some cases decreased in size (○). Tumors in L428$^{tetPU.1}$ (C) and KM-H2$^{tetPU.1}$ (D) xenografts did not grow after tetracycline withdrawal. Left panels: Tumors in a xenograft mouse taking tetracycline water. Right panel: Tumors after tetracycline withdrawal. Survival curves of L428$^{tetPU.1}$ (E) and KM-H2$^{tetPU.1}$ (F) xenograft mice. L428$^{tetPU.1}$ xenograft mice taking tetracycline all died within 96 days, whereas 7 of 8 mice without tetracycline survived > 190 days. KM-H2$^{tetPU.1}$ xenograft mice taking tetracycline all died within 143 days, whereas 6 of 8 mice without tetracycline survived > 155 days.

of L428$^{tetPU.1}$ and KM-H2$^{tetPU.1}$ cells 0, 1, and 3 days after PU.1 induction, by DNA microarray. In the case of L428$^{tetPU.1}$ cells, the top 30 genes up-regulated and down-regulated at day 1 and day 3 are shown in supplemental Tables 1 through 4. Genes up-regulated 24 hours after PU.1 induction (> 8-fold at day 1) are shown in Figure 5A. These genes contain IFN-stimulated genes (ISGs), including *TRIM22*, *IFI44L*, and *OAS3*. We previously reported that ISGs, including *IFIT1*, *IFITM1*, *IFIT2*, *IFIT4*, *IFI27*, *ISG15*, *LY6E*, and *IFI6*, were up-regulated in the multiple myeloma cell line, U266, after induction of PU.1 expression using the same tet-off system. IRF7, a key transcription factor involved in IFN signal transduction, was also highly up-regulated as previously shown in U266 cells expressing PU.1. Within the category of genes related to cell cycle or apoptosis, we observed that *p21 (CDKN1A)* was highly up-regulated at day 1 and day 3 after PU.1 induction, and this was confirmed by real-time PCR and Western blot (Figure 5B-C).

To clarify the role of p21 up-regulation in Hodgkin lymphoma cell growth, we stably silenced p21 in L428$^{tetPU.1}$ cells using siRNA. p21 siRNA strongly suppressed p21 expression in L428$^{tetPU.1}$ cells, before and after PU.1 induction (Figure 6A). Stable knockdown of p21 rescued L428$^{tetPU.1}$ cells from growth arrest induced by PU.1 (Figure 6B). Taken together, these data suggest that L428$^{tetPU.1}$ growth arrest induced by PU.1 is at least partially dependent on p21 up-regulation.

In the case of KM-H2$^{tetPU.1}$ cells, genes up-regulated after PU.1 induction (> 10-fold at day 1) are shown in supplemental Figure 2. The top 30 genes up-regulated and down-regulated one or 3 days after PU.1 induction are shown in supplemental Tables 5 through 8. *p21* was not included in these genes. Indeed, p21 was not up-regulated at the protein level after PU.1 induction, whereas *p21* mRNA was up-regulated 6-fold (Figure 5B-C). Therefore, the mechanisms underlying cell-cycle arrest in KH-M2$^{tetPU.1}$ cells expressing PU.1 may be distinct from those of L428$^{tetPU.1}$ cells expressing PU.1. There were no highly up-regulated ISGs; however, *IRF7* was highly up-regulated at both day 1 (13-fold) and day 3 (14.6-fold). Among genes related to the immune system, *IL1RN*, *LILRA3*, *IGDCC3*, and *LILRA2* were highly up-regulated both at day 1 and day 3. Within the category of genes related to cell cycle or apoptosis, *Aurora kinase C* and *FGFR4* were highly up-regulated one and 3 days after PU.1 induction. Among down-regulated genes that may be related to cell cycle or apoptosis, *PRDM1* and *TNFRSF18* were highly down-regulated at day 1 after PU.1 induction. Notably, PRDM1 is a key transcription factor involved in late B-cell differentiation; however, down-regulation of *PRDM1* was not sustained (0.9-fold) 3 days after PU.1 induction. Further studies are required to elucidate the role of these genes in cell-cycle arrest and apoptosis observed in KM-H2 $^{tetPU.1}$ cells after PU.1 induction.

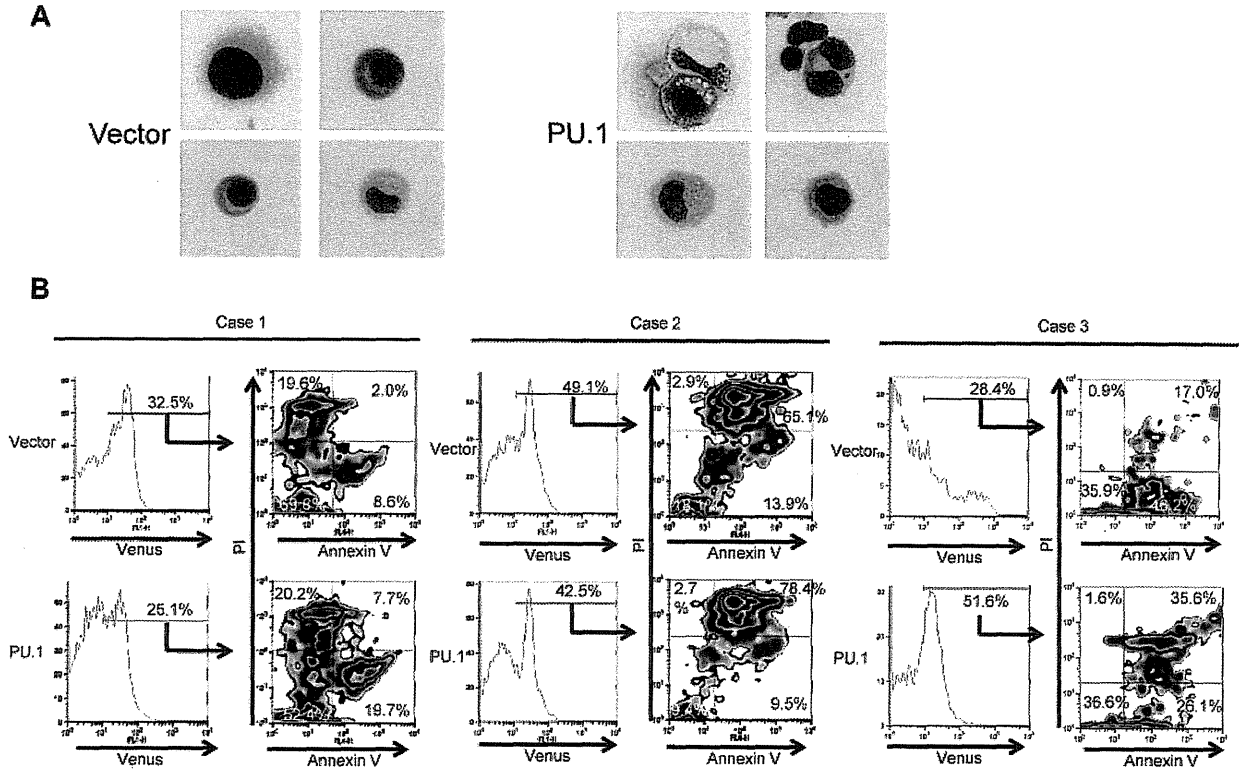

Figure 4. PU.1 induces apoptosis in primary cHL cells from patients. (A) Morphology of purified, primary cHL cells transduced with control lentivirus (Case 1, 4 left panels) or PU.1 expressing lentivirus (Case 1, 4 right panels). A number of primary classic Hodgkin cells expressing PU.1 contained various-sized vacuoles Images were acquired using a BX60 microscope and DP70 digital camera with DP controller software (Olympus; ×1000 magnification). (B) Primary cHL cells transduced with PU.1 lentivirus tended to undergo apoptosis compared with cells transduced with empty vector. Apoptosis was assessed in Venus-positive cells by flow cytometry after staining with PI and allophycocyanin-conjugated annexin V. Stable transduction of primary cHL cells from case 1 with PU.1 lentivirus led to a decrease in the percentage of live PI^-/annexin V^- cells and an increased percentage of PI^-/annexin V^+ preapoptotic cells, compared with control vector. Stable transduction of primary cHL cells from case 2 with PU.1 lentivirus also led to a decrease in the percentage of live PI^-/annexin V^- cells and an increased percentage of PI^+ apoptotic cells. Stable transduction of primary cHL cells from case 3 with PU.1 lentivirus also led to a decrease in the percentage of live PI^-/annexin V^+ cells and an increased percentage of PI^+ apoptotic cells.

5-aza-2′-deoxycytidine and/or trichostatin A induces up-regulation of PU.1 and apoptosis in cHL cells

Given that PU.1 is down-regulated in Hodgkin lymphoma cells by promoter and URE methylation, and that overexpression of PU.1 induced growth arrest and apoptosis of Hodgkin lymphoma cells, we hypothesized that up-regulation of PU.1 after treatment with demethylation agents and/or histone deacetylase (HDAC) inhibitors might represent a new therapeutic modality for Hodgkin lymphoma patients. We first evaluated the ability of 5-aza-2′-deoxycytidine to induce PU.1 expression. Treatment of Hodgkin lymphoma cell lines with 1μM 5-aza-2′-deoxycytidine induced *PU.1* mRNA expression in HD-70, L540, HDLM2, and KM-H2 cells but not in L428 cells (Figure 7A).

We next evaluated the ability of HDAC inhibitors to induce PU.1 expression. Whereas treatment with SAHA failed to induce *PU.1* expression in either L428, KM-H2 cells, trichostatin A induced expression of *PU.1* mRNA in KM-H2 cells, but not in L428 cells (data not shown). We also evaluated the effect of combined treatment with both 5-aza-2′-deoxycytidine and trichostatin A on cell growth and apoptosis in Hodgkin lymphoma cell lines. Treatment of L428 cells with 1μM 5-aza-2′-deoxycytidine and 500nM trichostatin A led to induction of *PU.1* mRNA expression (Figure 7A right panel). We next evaluated the effects of these agents on these Hodgkin lymphoma cell growth. Treatment with 1μM 5-aza-2′-deoxycytidine induced growth arrest in HD-70, L540, HDLM2, and KM-H2 cells (Figure 7B-E); however, L428 cells remained unaffected after treatment with 1μM 5-aza-2′-deoxycytidine (Figure 7F). In contrast, the combination of 1μM 5-aza-2′-deoxycytidine and 500nM trichostatin A induced growth arrest in L428 cells (Figure 7G). Given that the combination of 5-aza-2′-deoxycytidine and trichostatin A, but not treatment with 5-aza-2′-deoxycytidine alone, was capable of inducing PU.1 expression and growth arrest in L428 cells, these results indicate that PU.1 is at least partially responsible for inducing growth arrest of L428 cells in this setting. These data suggest that up-regulation of PU.1 by demethylation agents and HDAC inhibitors may represent a new therapeutic strategy for the treatment of cHL.

Discussion

In this study, we present data demonstrating that PU.1 is a potent tumor suppressor in cHL. First, using bisulfite sequencing, we showed that PU.1 is silenced by the methylation of its promoter and a −17 kb URE. Next, we demonstrated that PU.1 induced growth arrest and apoptosis in cHL cell lines, L428 and KM-H2, and primary cHL cells in vitro. In addition, using a xenograft mouse model harboring tumors of L428 or KM-H2 cells, we showed that PU.1 up-regulation induced tumor regression and promoted long-term survival, compared with mice without PU.1 induction. Finally, we showed that, in the case of L428 cells, growth arrest induced by PU.1 was mediated, at least in part, by the up-regulation of p21.

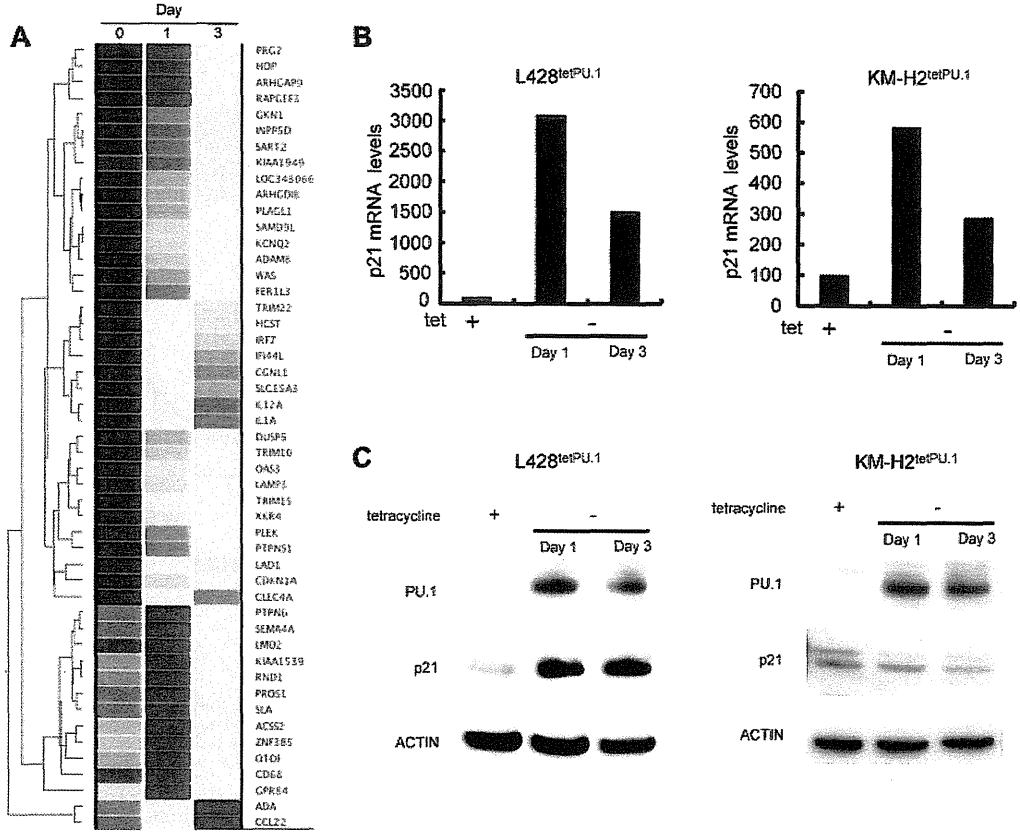

Figure 5. p21 is highly up-regulated in L428$^{tetPU.1}$ cells after PU.1 induction. (A) Heatmap of DNA microarray analysis comparing the gene expression profiles of L428$^{tetPU.1}$ cells after PU.1 induction at days 0, 1, and 3. *p21 (CDKN1A)* mRNA was highly up-regulated after PU.1 induction. (B) *p21* mRNA was up-regulated in both L428$^{tetPU.1}$ and KM-H2$^{tetPU.1}$ cells after PU.1 induction. Real-time PCR was performed 1 and 3 days after PU.1 induction. (C) p21 protein was up-regulated in L428$^{tetPU.1}$ but not in KM-H2$^{tetPU.1}$ cells after PU.1 induction. Western blot for p21, PU.1, and actin was performed 1 and 3 days after PU.1 induction.

The oncogenic mechanisms underlying cHL are not well understood. Many B cell–specific genes are down-regulated in cHL cells, including B cell–specific transcription factors, Oct2, Bob1, and PU.1, and cell surface markers, CD19, CD20, and CD79.[15] Down-regulation of these genes is caused by promoter methylation.[23] In contrast, cHL cells express CD30, a marker expressed on activated B cells and T cells. However, to date, the significance of the down-regulation of B cell–specific genes and the expression of CD30 in cHL remain enigmatic.

One of the genetic lesions of cHL is constitutive activation of the canonical nuclear factor of κ light polypeptide gene enhancer in B-cells (NF-κB) pathway.[37] A recent report showed that TNFAIP3 (A20), a negative regulator of the NFκB pathway, is inactivated by deletions and somatic mutations in 40% of cHL patients and in the cHL cell line, KM-H2.[13] In addition to TNFAIP3, somatic mutations of *NFκBIA*, which also inhibits the NF-κB signaling pathway, have been identified in KM-H2 cells.[37] *NFκBIA*, also known as IκB, is mutated in ~ 20% of cHL patients.[37-40] It is also well documented that ~ 50% of cHL patients harbor amplification or gain of *REL*, which is a component of NFκB.[41-43] Taken together, these data indicate that constitutive activation of NFκB is a key event underlying the pathogenesis of cHL. Our microarray analysis of L428$^{tetPU.1}$ cells revealed that PU.1 induced a 2- to 3-fold

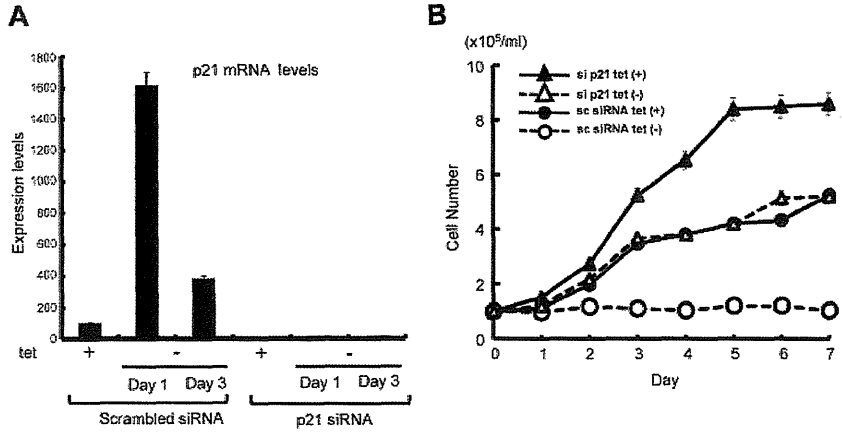

Figure 6. PU.1-induced cell growth arrest in L428$^{tetPU.1}$ cells is dependent on p21 up-regulation. (A) Stable knockdown of p21 strongly suppressed p21 expression, even after PU.1 induction in L428$^{tetPU.1}$ cells. (B) The growth arrest of L428$^{tetPU.1}$ cells induced by PU.1 overexpression was reversed by targeted knockdown of p21. PU.1-induced growth arrest in L428$^{tetPU.1}$ cells stably transduced with scrambled siRNA (○), whereas PU.1 failed to induce growth arrest in L428$^{tetPU.1}$ cells stably transduced with p21 siRNA (△).

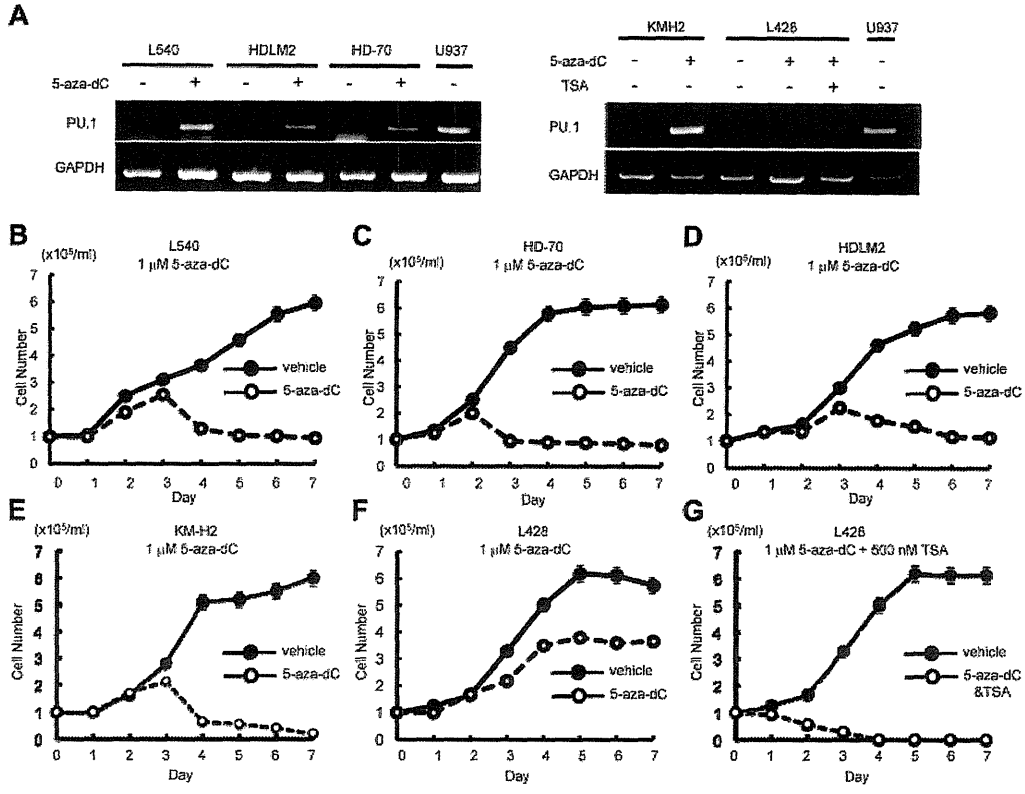

Figure 7. Individual or combined treatment with demethylation agent and HDAC inhibitors is a possible therapeutic strategy for cHL. (A) 5-aza-2′-deoxycytidine and/or trichostatin A (TSA) induced PU.1 expression in cHL cell lines. Treatment of L540, HDLM2, HD-70, and KM-H2 cells with 1 μM 5-aza-2′-deoxycytidine induced PU.1 expression after 3 days. In contrast, treatment of L428 cells with 1 μM 5-aza-2′-deoxycytidine failed to induce PU.1 expression, whereas the combined treatment with 1 μM 5-aza-2′-deoxycytidine and 500nM TSA led to induction of PU.1 expression after 3 days. (B-E) Treatment of L540 (B), HD-70 (C), HDLM2 (D), and KM-H2 (E) cells with 1 μM 5-aza-2′-deoxycytidine induced growth arrest. (F) Treatment of L428 cells with 1 μM 5-aza-2′-deoxycytidine failed to induce growth arrest. (G) The combined treatment of L428 cells with 1 μM 5-aza-2′-deoxycytidine and 500nM of TSA induced growth arrest.

up-regulation of TNFAIP3 at both 1 and 3 days (data not shown). Up-regulation of TNFAIP3 may block the NFκB pathway, therefore accounting for the observed cell-cycle arrest and apoptosis in L428 $^{tetPU.1}$ cells after PU.1 induction. In contrast, we did not observe any significant change in the expression of NFκB composite proteins (> 2-fold) in L428$^{tetPU.1}$ cells after PU.1 induction, indicating that PU.1 does not affect the expression of composite members of the NFκB protein complex.

In this study, we also elucidated the mechanisms of L428$^{tetPU.1}$ and KM-H2$^{tetPU.1}$ cell growth arrest after PU.1 induction. Gene expression profiling of L428$^{tetPU.1}$ cells after induction of PU.1 revealed up-regulation of p21, and this accounted at least in part for the cell growth arrest. These results are very similar to our previous finding that p21 is up-regulated by PU.1, leading to cell-cycle arrest in the U266 myeloma cell line.[27] Therefore, loss of p21 expression may be involved in the dysregulation of cell growth in some subsets of B-cell malignancies that have lost PU.1 expression. In contrast, the KM-H2 Hodgkin lymphoma cell line did not display p21 up-regulation at the protein level after PU.1 induction. Thus, up-regulation of p21 does not explain the growth arrest observed after PU.1 induction in all subsets of B-cell malignancies. In the case of apoptosis, we previously reported that PU.1 induces apoptosis in U266 myeloma cells via up-regulation of the TNF-related apoptosis inducing ligand.[27] Nevertheless, TNF-related apoptosis inducing ligand was intrinsically highly expressed in L428$^{tetPU.1}$ and KM-H2 $^{tetPU.1}$ cells in the absence of PU.1 expression, and PU.1 did not further induce TNF-related apoptosis inducing ligand expression in either cell line. Therefore, the mechanism of apoptosis induced by PU.1 in these Hodgkin lymphoma cell lines is probably different from that observed in U266 myeloma cells. The identification of downstream effector proteins involved in PU.1-induced apoptosis in cHL cells may therefore provide new molecular targets for therapy in these patients.

In conclusion, we show that up-regulation of PU.1 in cHL cells induces cell-cycle arrest and apoptosis in vitro and in vivo, and demonstrate that cell-cycle arrest is accounted for, at least partially, by up-regulation of p21. Based on these data, it is possible that demethylation agents and HDAC inhibitors, which induce PU.1 up-regulation, may represent new molecular target modalities for treatment of patients with cHL.

Acknowledgments

This work was supported by the Ministry of Education, Culture, Sports, Science and Technology of Japan.

Authorship

Contribution: H.Y. conducted the majority of experiments, generated KM-H2$^{tetPU.1}$ cells and the xenograft model mice, and wrote the manuscript; S.U. isolated mRNA for DNA microarray analysis; H.T. designed the project; S.E. performed lentiviral transduction and flow cytometry; Y. Kawano analyzed survival curves of xenograft mice; H.N., T.I., and K.A. performed DNA microarray

analysis; Y. Komohara and M.T. performed immunostaining of primary Hodgkin lymphoma cells; H.H., T.W., and H.M. gave useful advice; S.O. generated *Rag2*$^{-/-}$*Jak3*$^{-/-}$ *balb/c* mice and gave useful advice to generate xenograft mice; and Y.O. designed the project, generated L428$^{tetPU.1}$ cells, and wrote manuscript.

Conflict-of-interest disclosure: The authors declare no competing financial interests.

Correspondence: Yutaka Okuno, Department of Hematology, Kumamoto University of Medicine, 1-1-1 Honjo, Kumamoto 860-8556, Japan; e-mail: yokuno@gpo.kumamoto-u.ac.jp.

References

1. Chan J, Jaffe E, Ralfkiaer E, Ko Y. *WHO Classification of Tumours of Haematopoietic and Lymphoid Tissues.* 4th Ed. Lyon, France: IARC Press; 2008.
2. Meyer RM, Gospodarowicz MK, Connors JM, et al. ABVD alone versus radiation-based therapy in limited-stage Hodgkin's lymphoma. *N Engl J Med.* 2012;366(5):399-408.
3. von Tresckow B, Plutschow A, Fuchs M, et al. Dose-intensification in early unfavorable Hodgkin's lymphoma: final analysis of the German Hodgkin Study Group HD14 Trial. *J Clin Oncol.* 2012;30(9):907-913.
4. Viviani S, Zinzani PL, Rambaldi A, et al. ABVD versus BEACOPP for Hodgkin's lymphoma when high-dose salvage is planned. *N Engl J Med.* 2011;365(3):203-212.
5. Chisesi T, Bellei M, Luminari S, et al. Long-term follow-up analysis of HD9601 trial comparing ABVD versus Stanford V versus MOPP/EBV/CAD in patients with newly diagnosed advanced-stage Hodgkin's lymphoma: a study from the Intergruppo Italiano Linfomi. *J Clin Oncol.* 2011;29(32):4227-4233.
6. Borchmann P, Haverkamp H, Diehl V, et al. Eight cycles of escalated-dose BEACOPP compared with four cycles of escalated-dose BEACOPP followed by four cycles of baseline-dose BEACOPP with or without radiotherapy in patients with advanced-stage Hodgkin's lymphoma: final analysis of the HD12 trial of the German Hodgkin Study Group. *J Clin Oncol.* 2011;29(32):4234-4242.
7. Halbsguth T, Nogova L, Mueller H, et al. Phase 2 study of BACOPP (bleomycin, adriamycin, cyclophosphamide, vincristine, procarbazine, and prednisone) in older patients with Hodgkin lymphoma: a report from the German Hodgkin Study Group (GHSG). *Blood.* 2010;116(12):2026-2032.
8. Eich H, Diehl V, Gorgen H, et al. Intensified chemotherapy and dose-reduced involved-field radiotherapy in patients with early unfavorable Hodgkin's lymphoma: final analysis of the German Hodgkin Study Group HD11 trial. *J Clin Oncol.* 2010;28(27):4199-4206.
9. Engert A, Diehl V, Franklin J, et al. Escalated-dose BEACOPP in the treatment of patients with advanced-stage Hodgkin's lymphoma: 10 years of follow-up of the GHSG HD9 study. *J Clin Oncol.* 2009;27(27):4548-4554.
10. Engert A, Plutschow A, Eich HT, et al. Reduced treatment intensity in patients with early-stage Hodgkin's lymphoma. *N Engl J Med.* 2010;363(7):640-652.
11. van der Kaaij MA, Heutte N, Meijnders P, et al. Premature ovarian failure and fertility in long-term survivors of Hodgkin's lymphoma: a European Organisation for Research and Treatment of Cancer Lymphoma Group and Groupe d'Etude des Lymphomes de l'Adulte Cohort Study. *J Clin Oncol.* 2012;30(3):291-299.
12. Swerdlow AJ, Higgins CD, Smith P, et al. Second cancer risk after chemotherapy for Hodgkin's lymphoma: a collaborative British cohort study. *J Clin Oncol.* 2011;29(31):4096-4104.
13. Kato M, Sanada M, Kato I, et al. Frequent inactivation of A20 in B-cell lymphomas. *Nature.* 2009;459(7247):712-716.
14. Jundt F, Kley K, Anagnostopoulos I, et al. Loss of PU.1 expression is associated with defective immunoglobulin transcription in Hodgkin and Reed-Sternberg cells of classical Hodgkin disease. *Blood.* 2002;99(8):3060-3062.
15. McCune R, Syrbu S, Vasef M. Expression profiling of transcription factors Pax-5, Oct-1, Oct-2, BOB. 1, and PU.1 in Hodgkin's and non-Hodgkin's lymphomas: a comparative study using high throughput tissue microarrays. *Mod Pathol.* 2006;19(7):1010-1018.
16. Scott EW, Simon MC, Anastasi J, Singh H. Requirement of transcription factor PU.1 in the development of multiple hematopoietic lineages. *Science.* 1994;265(5178):1573-1577.
17. McKercher SR, Torbett BE, Anderson KL, et al. Targeted disruption of the PU.1 gene results in multiple hematopoietic abnormalities. *EMBO J.* 1996;15(20):5647-5658.
18. Li Y, Okuno Y, Zhang P, et al. Regulation of the PU.1 gene by distal elements. *Blood.* 2001;98(10):2958-2965.
19. Okuno Y, Huang G, Rosenbauer F, et al. Potential autoregulation of transcription factor PU.1 by an upstream regulatory element. *Mol Cell Biol.* 2005;25(7):2832-2845.
20. Tatetsu H, Ueno S, Hata H, et al. Down-regulation of PU.1 by methylation of distal regulatory elements and the promoter is required for myeloma cell growth. *Cancer Res.* 2007;67(11):5328-5336.
21. Rosenbauer F, Wagner K, Kutok JL, et al. Acute myeloid leukemia induced by graded reduction of a lineage-specific transcription factor, PU.1. *Nat Genet.* 2004;36(6):624-630.
22. Rosenbauer F, Owens BM, Yu L, et al. Lymphoid cell growth and transformation are suppressed by a key regulatory element of the gene encoding PU.1. *Nat Genet.* 2006;38(1):27-37.
23. Ushmorov A, Leithauser F, Sakk O, et al. Epigenetic processes play a major role in B-cell-specific gene silencing in classical Hodgkin lymphoma. *Blood.* 2006;107(6):2493-2500.
24. Era T, Witte ON. Regulated expression of P210 Bcr-Abl during embryonic stem cell differentiation stimulates multipotential progenitor expansion and myeloid cell fate. *Proc Natl Acad Sci U S A.* 2000;97(4):1737-1742.
25. Miyoshi H, Takahashi M, Gage FH, Verma IM. Stable and efficient gene transfer into the retina using an HIV-based lentiviral vector. *Proc Natl Acad Sci U S A.* 1997;94(19):10319-10323.
26. Miyoshi H, Blomer U, Takahashi M, Gage FH, Verma IM. Development of a self-inactivating lentivirus vector. *J Virol.* 1998;72(10):8150-8157.
27. Ueno S, Tatetsu H, Hata H, et al. PU.1 induces apoptosis in myeloma cells through direct transactivation of TRAIL. *Oncogene.* 2009;28(46):4116-4125.
28. Dolbeare F, Gratzner H, Pallavicini MG, Gray JW. Flow cytometric measurement of total DNA content and incorporated bromodeoxyuridine. *Proc Natl Acad Sci U S A.* 1983;80(18):5573-5577.
29. Peterson KR, Clegg CH, Huxley C, et al. Transgenic mice containing a 248-kb yeast artificial chromosome carrying the human beta-globin locus display proper developmental control of human globin genes. *Proc Natl Acad Sci U S A.* 1993;90(16):7593-7597.
30. Kaufman RM, Pham CT, Ley TJ. Transgenic analysis of a 100-kb human beta-globin cluster-containing DNA fragment propagated as a bacterial artificial chromosome. *Blood.* 1999;94(9):3178-3184.
31. Tanimoto K, Liu Q, Bungert J, Engel JD. Effects of altered gene order or orientation of the locus control region on human beta-globin gene expression in mice. *Nature.* 1999;398(6725):344-348.
32. Yu W, Misulovin Z, Suh H, et al. Coordinate regulation of RAG1 and RAG2 by cell type-specific DNA elements 5′ of RAG2. *Science.* 1999;285(5430):1080-1084.
33. Loots GG, Locksley RM, Blankespoor CM, et al. Identification of a coordinate regulator of interleukins 4, 13, and 5 by cross-species sequence comparisons. *Science.* 2000;288(5463):136-140.
34. Okuno Y, Iwasaki H, Huettner CS, et al. Differential regulation of the human and murine CD34 genes in hematopoietic stem cells. *Proc Natl Acad Sci U S A.* 2002;99(9):6246-6251.
35. Okuno Y, Huettner CS, Radomska HS, et al. Distal elements are critical for human CD34 expression in vivo. *Blood.* 2002;100(13):4420-4426.
36. Radomska HS, Gonzalez DA, Okuno Y, et al. Transgenic targeting with regulatory elements of the human CD34 gene. *Blood.* 2002;100(13):4410-4419.
37. Kuppers R. The biology of Hodgkin's lymphoma. *Nat Rev Cancer.* 2009;9(1):15-27.
38. Cabannes E, Khan G, Aillet F, Jarrett R, Hay R. Mutations in the IkBa gene in Hodgkin's disease suggest a tumour suppressor role for IkappaBalpha. *Oncogene.* 1999;18(20):3063-3070.
39. Emmerich F, Meiser M, Hummel M, et al. Overexpression of I kappa B alpha without inhibition of NF-kappaB activity and mutations in the I kappa B alpha gene in Reed-Sternberg cells. *Blood.* 1999;94(9):3129-3134.
40. Jungnickel B, Staratschek-Jox A, Brauninger A, et al. Clonal deleterious mutations in the IkappaBalpha gene in the malignant cells in Hodgkin's lymphoma. *J Exp Med.* 2000;191(2):395-402.
41. Barth T, Martin-Subero J, Joos S, et al. Gains of 2p involving the REL locus correlate with nuclear c-Rel protein accumulation in neoplastic cells of classical Hodgkin lymphoma. *Blood.* 2003;101(9):3681-3686.
42. Joos S, Menz C, Wrobel G, et al. Classical Hodgkin lymphoma is characterized by recurrent copy number gains of the short arm of chromosome 2. *Blood.* 2002;99(4):1381-1387.
43. Martin-Subero J, Gesk S, Harder L, et al. Recurrent involvement of the REL and BCL11A loci in classical Hodgkin lymphoma. *Blood.* 2002;99(4):1474-1477.

Brief report

Plasma biomarkers of lower gastrointestinal and liver acute GVHD

Andrew C. Harris,[1] James L. M. Ferrara,[1] Thomas M. Braun,[2] Ernst Holler,[3] Takanori Teshima,[4] John E. Levine,[1] Sung W. Choi,[1] Karin Landfried,[3] Koichi Akashi,[4] Mark Vander Lugt,[1] Daniel R. Couriel,[1] Pavan Reddy,[1] and Sophie Paczesny[1]

[1]Blood and Marrow Transplant Program and [2]Department of Biostatistics, The University of Michigan, Ann Arbor, MI; [3]Department of Hematology/Oncology, University Medical Center Regensburg, Regensburg, Germany; and [4]Center for Cellular and Molecular Medicine, Kyushu University Graduate School of Science, Fukuoka, Japan

The lower gastrointestinal tract (LGI) and liver are the GVHD target organs most associated with treatment failure and nonrelapse mortality. We recently identified regenerating islet-derived 3-α (REG3α) as a plasma biomarker of LGI GVHD. We compared REG3α with 2 previously reported GI and liver GVHD diagnostic biomarkers, hepatocyte growth factor (HGF) and cytokeratin fragment 18, in 954 hematopoietic cell transplantation patients. All 3 biomarkers were significantly elevated in LGI GVHD compared with non-GVHD diarrhea; REG3α discerned LGI GVHD from non-GVHD diarrhea better than HGF and cytokeratin fragment 18. Although all 3 biomarkers predicted nonresponse to therapy at day 28 in LGI GVHD patients, only REG3α and HGF concentrations predicted 1-year nonrelapse mortality ($P = .01$ and $P = .02$, respectively). Liver GVHD without GI involvement at GVHD onset and non-GVHD liver complications were uncommon; all 3 biomarkers were elevated in liver GVHD, but did not distinguish GVHD from other causes of hyperbilirubinemia. (*Blood*. 2012;119(12): 2960-2963)

Introduction

Acute GVHD, a leading cause of nonrelapse mortality (NRM) after allogeneic hematopoietic cell transplantation (HCT), is measured by dysfunction in the skin, liver, and gastrointestinal (GI) tract.[1-3] We recently identified regenerating islet-derived 3-α (REG3α), an antimicrobial protein expressed in Paneth cells, as a biomarker of GVHD of the lower GI (LGI) tract that can differentiate LGI GVHD from non-GVHD diarrhea. Concentrations of this biomarker at onset of GVHD can predict response to treatment and NRM.[4] Hepatocyte growth factor (HGF) has been reported as a biomarker that is elevated in GVHD of the GI tract and liver as part of a panel of 4 GVHD biomarkers.[5] Similarly, cytokeratin fragment 18 (KRT18), an apoptotic protein, was described previously as a biomarker of visceral GVHD in a cohort of 55 patients,[6] and has recently been correlated with response to GVHD therapy.[7] Liver involvement has been historically observed in up to 36% of GVHD patients,[8,9] although a recent cohort demonstrated a declining incidence.[10] Liver involvement at GVHD onset occurs in 6%-20% of patients[8,9,11] and has been associated with poor response to GVHD therapy and increased NRM.[8,9,12] There are no validated biomarkers specific to liver GVHD. We compared the diagnostic and prognostic utility of REG3α, HGF, and KRT18 for LGI and liver GVHD.

Methods

Patients and samples

All plasma/serum samples and patient information were collected after obtaining patient consent in accordance with the Declaration of Helsinki for institutional review board–approved studies at the University of Michigan (n = 826), Regensburg, Germany (n = 88), and Kyushu, Japan (n = 40) for patients receiving HCT between January 2000 and November 2010, as described previously (and see supplemental Methods, available on the *Blood* Web site; see the Supplemental Materials link at the top of the online article).[4] Patients were divided into 6 groups: (1) patients with newly diagnosed GVHD diarrhea with or without skin involvement but without liver involvement (LGI GVHD), (2) patients with diarrhea inconsistent with GVHD either by clinical or histologic criteria (non-GVHD diarrhea), (3) patients with liver GVHD with or without skin involvement but without GI involvement (liver GVHD), (4) patients with liver complications attributable to non-GVHD causes (non-GVHD liver), (5) patients who presented with isolated skin GVHD (skin GVHD), and (6) patients at similar time points who never developed GVHD symptoms (no GVHD). Patient numbers and characteristics are shown in Table 1 and in supplemental Methods. Non-GVHD liver complications were included if patients never developed acute GVHD and experienced hyperbilirubinemia within 120 days of HCT in the absence of chronic GVHD. Causes of non-GVHD diarrhea and liver complications are described in supplemental Table 1. All samples were obtained at GVHD onset within 48 hours of initiation of systemic GVHD therapy and 1 sample was analyzed per patient. Patients who had non-GVHD complications before GVHD onset had samples evaluated only at GVHD onset. The rare incidence of liver involvement at GVHD onset did not permit analysis of 2 independent validation sets as was performed for REG3α in LGI GVHD.[4]

ELISAs

KRT18 ELISA kits were purchased from Peviva AB (M30 Apoptosense ELISA) and performed according to manufacturer protocol. Samples (diluted 1:2) and standards were run in duplicate. Absorbance was measured with a SpectraMax M2 (Molecular Devices), and results were calculated with SoftMax Pro Version 5.4 software (Molecular Devices).

Submitted October 20, 2011; accepted January 23, 2012. Prepublished online as *Blood* First Edition paper, January 27, 2012; DOI 10.1182/blood-2011-10-387357.

The online version of this article contains a data supplement.

The publication costs of this article were defrayed in part by page charge payment. Therefore, and solely to indicate this fact, this article is hereby marked "advertisement" in accordance with 18 USC section 1734.

Table 1. HCT patient characteristics (N = 954)

	LGI GVHD (n = 144)†	Non-GVHD diarrhea (n = 42)	Liver GVHD (n = 16)†	Non-GVHD liver (n = 25)	Skin GVHD (n = 337)	No GVHD (n = 390)	*P*
Age, y							
Median (range)	52 (0-67)	46 (3-66)	44 (19-63)	35 (0-64)	48 (0-70)	46 (0-68)	.001
Disease							
Malignant	94% (n = 135)	86% (n = 36)	100% (n = 16)	80% (n = 20)	94% (n = 317)	88% (n = 342)	.005
Other	6% (n = 9)	14% (n = 6)	0% (n = 0)	20% (n = 5)	6% (n = 20)	12% (n = 48)	
Disease status at transplantation*							
Low-/intermediate-risk	59% (n = 79)	67% (n = 24)	44% (n = 7)	75% (n = 15)	65% (n = 205)	66% (n = 226)	.3
High-risk	41% (n = 56)	33% (n = 12)	56% (n = 9)	25% (n = 5)	35% (n = 112)	34% (n = 116)	
Donor type							
Related donor	42% (n = 60)	52% (n = 22)	56% (n = 9)	68% (n = 17)	37% (n = 124)	58% (n = 228)	< .001
Unrelated donor	58% (n = 84)	48% (n = 20)	44% (n = 7)	32% (n = 8)	63% (n = 213)	42% (n = 162)	
Donor match							
Matched donor	71% (n = 102)	93% (n = 39)	81% (n = 13)	88% (n = 22)	73% (n = 245)	89% (n = 346)	< .001
Mismatched donor	29% (n = 42)	7% (n = 3)	19% (n = 3)	12% (n = 3)	27% (n = 92)	11% (n = 44)	
Conditioning regimen intensity							
High-intensity	53% (n = 77)	64% (n = 27)	69% (n = 11)	84% (n = 21)	54% (n = 181)	61% (n = 239)	.02
Moderate-intensity	47% (n = 67)	36% (n =15)	31% (n = 5)	16% (n = 4)	46% (n = 156)	39% (n = 151)	
Grade of GVHD at onset							
Grade 0	0% (n = 0)	100% (n = 42)	0% (n = 0)	100% (n = 25)	0% (n = 0)	100% (n = 390)	
Grade I	0% (n = 0)	0% (n = 0)	0% (n = 0)	0% (n = 0)	69% (n = 231)	0% (n = 0)	
Isolated skin stage 1	0% (n = 0)	0% (n = 0)	0% (n = 0)	0% (n = 0)	38% (n = 129)	0% (n = 0)	
Isolated skin stage 2	0% (n = 0)	0% (n = 0)	0% (n = 0)	0% (n = 0)	30% (n = 102)	0% (n = 0)	
Grade II	52% (n = 75)	0% (n = 0)	44% (n = 7)	0% (n = 0)	31% (n = 105)	0% (n = 0)	
Isolated skin stage 3	0% (n = 0)	0% (n = 0)	0% (n = 0)	0% (n = 0)	31% (n = 105)	0% (n = 0)	
GI or liver stage 1	52% (n = 75)†	0% (n = 0)	44% (n = 7)	0% (n = 0)	0% (n = 0)	0% (n = 0)	
Grade III-IV	48% (n = 69)	0% (n = 0)	56% (n = 9)	0% (n = 0)	< 1% (n = 1)	0% (n = 0)	
Isolated skin stage 4	0% (n = 0)	0% (n = 0)	0% (n = 0)	0% (n = 0)	< 1% (n = 1)	0% (n = 0)	
GI or liver stage 2	17% (n = 24)†	0% (n = 0)	38% (n = 6)	0% (n = 0)	0% (n = 0)	0% (n = 0)	
GI or liver stage 3	18% (n = 26)†	0% (n = 0)	13% (n = 2)	0% (n = 0)	0% (n = 0)	0% (n = 0)	
GI or liver stage 4	13% (n = 19)†	0% (n = 0)	6% (n = 1)	0% (n = 0)	0% (n = 0)	0% (n = 0)	
Days after HCT							
Median (range)	30 (7-215)	21 (7-78)	33 (10-112)	21 (7-106)	28 (5-485)	30 (7-185)	< .001

*High risk of disease status at HCT is according to Center for International Blood and Marrow Transplant Research guidelines.
†With or without skin GVHD involvement.

Other biomarker ELISAs were performed as described previously (and see supplemental Methods).[4,5]

Statistical analysis

Biomarker concentrations from individual patient samples were compared using 2-sample *t* tests applied to log-transformed concentrations. Differences in characteristics between patient groups were assessed with a Kruskal-Wallis test for continuous values and χ^2 tests of association for categorical values. Receiver operating characteristic (ROC) areas under the curve (AUCs) were estimated nonparametrically. NRM was modeled with cumulative incidence regression methods as described by Fine and Gray.[13]

Results and discussion

Biomarker concentrations were measured in samples from N = 954 allogeneic HCT recipients from the University of Michigan (n = 826), University Medical Center Regensburg (n = 88), and Kyushu University (n = 40; Table 1). The incidence of liver involvement at onset of GVHD requiring systemic corticosteroids (35 of 285; 12%) in our patient dataset was comparable to previous reports.[8,9,11,14] There was no statistical difference in biomarker concentrations based on GVHD prophylaxis whether a calcineurin inhibitor was combined with either methotrexate or mycophenolate mofetil (supplemental Table 2). All 3 biomarkers were significantly elevated in LGI GVHD compared with non-GVHD diarrhea and asymptomatic patients (Figure 1A-C). REG3α and HGF concentrations were also elevated in LGI GVHD compared with isolated skin GVHD, whereas KRT18 concentrations were not. This is consistent with the KRT18 tissue expression profile,[15] but differs from findings reported by Luft et al that KRT18 concentrations are not elevated in skin GVHD.[6]

We compared the diagnostic ability of REG3α, HGF, and KRT18 as biomarkers for LGI GVHD using ROC curves. REG3α performed better than KRT18 and HGF as a diagnostic biomarker distinguishing LGI GVHD from non-GVHD diarrhea (Figure 1D; AUC = 0.79, 0.60, and 0.60, respectively). The combination of all 3 biomarkers into a composite panel provided minimal additional diagnostic utility to that of REG3α alone (AUC = 0.80). Positive and negative predictive values for diagnostic utility of all 3 biomarkers are listed in supplemental Table 3. REG3α concentrations maintained diagnostic utility in patients experiencing diarrhea within 14 days of HCT, whereas HGF and KRT18 did not (supplemental Table 4). All 3 biomarkers, when measured at the onset of LGI GVHD, predicted nonresponse to therapy at 28 days[16-18] (supplemental Figure 1 and supplemental Table 5).

We divided patients into groups of equal size according to whether biomarker concentrations were above (high) or below (low) the median concentration at the onset of LGI GVHD. High REG3α and HGF concentrations correlated with significantly higher 1-year NRM, whereas there was no significant correlation

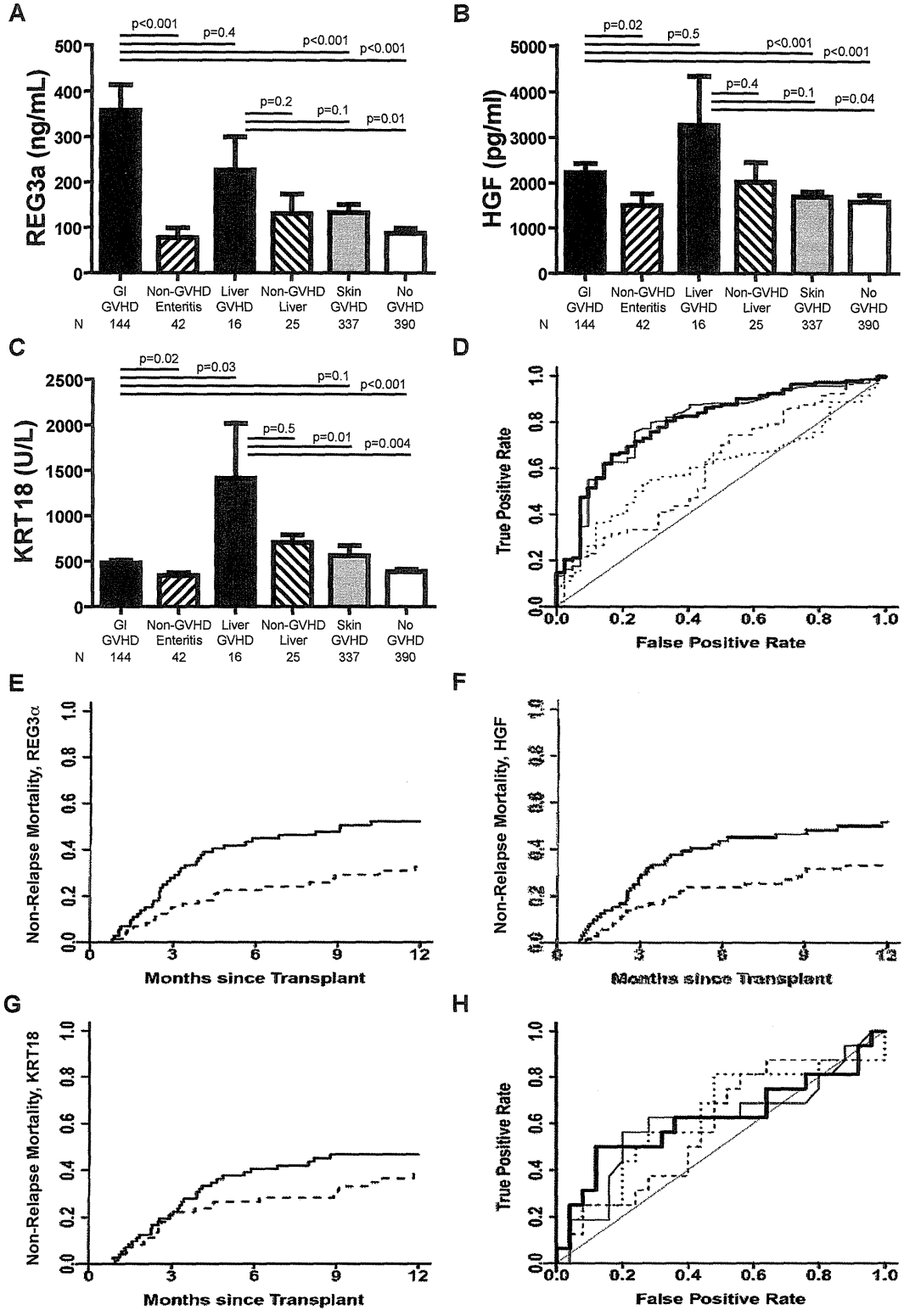

Figure 1. Biomarkers at the onset of GVHD symptoms. (A-C) REG3α, HGF, and KRT18 concentrations, respectively, at the onset of symptoms consistent with GVHD in 954 HCT patients. (D) ROC curves comparing biomarker concentrations at the onset of LGI GVHD without liver GVHD (n = 144) and non-GVHD diarrhea (n = 42). REG3α (thin solid line): AUC = 0.79; HGF (dotted line): AUC = 0.60; KRT18 (dashed line): AUC = 0.60; composite of all 3 biomarkers (thick solid line): AUC = 0.80. (E-G) NRM in patients with LGI GVHD at onset with onset concentrations above the median (solid line; n = 89) versus patients with onset concentrations below the median (dotted line; n = 89) for REG3a, HGF, and KRT18, respectively. (E) REG3a: > 135 ng/mL versus ≤ 135 ng/mL; 52% versus 33%, *P* = .01. (F) HGF: > 1398 pg/mL versus ≤ 1398 pg/mL; 52% versus 33%, *P* = .02. (G) KRT18 > 373 U/L versus ≤ 373 U/L; 47% versus 38%, *P* = .3. (H) ROC curves comparing biomarker concentrations at the onset of liver GVHD without GI GVHD (n = 16) and non-GVHD liver complications (n = 25); REG3α (thin solid line): AUC = 0.61; HGF (dotted line): AUC = 0.59; KRT18 (dashed line): AUC = 0.63; composite of all 3 biomarkers (thick solid line): AUC = 0.62.

between NRM and high KRT18 concentrations. (Figure 1E-G; $P = .01$, $P = .02$, and $P = .3$, respectively). Biomarker concentrations were comparable at onset between patients receiving systemic corticosteroids alone (n = 102) and those receiving multiagent therapy (n = 40) as initial GVHD treatment (supplemental Table 6).

In the present study and as reported recently,[10] liver GVHD without GI involvement at the onset of disease was uncommon (n = 16; 3% of GVHD patients and 2% of all patients), as were liver complications early after HCT (n = 25; 3% of all patients). REG3α and HGF concentrations were elevated in liver GVHD compared with asymptomatic patients, but were comparable to concentrations in patients with LGI GVHD, non-GVHD hyperbilirubinemia, and isolated skin GVHD (Figure 1A-B). KRT18 concentrations were significantly higher in patients with liver GVHD than in all other patients except those with non-GVHD liver complications (Figure 1C). None of the 3 biomarkers effectively distinguished liver GVHD from non-GVHD liver complications (Figure 1H; AUC = 0.61, 0.59, and 0.63, respectively; composite panel AUC = 0.62). Most patients with non-GVHD liver complications had sinusoidal obstruction syndrome (n = 20), which can often be distinguished clinically from GVHD. Cases in which biopsies were required to determine the etiology of hyperbilirubinemia during the period in which patients typically develop acute GVHD were very uncommon in our patient cohort (n = 7).

When including all patients with concomitant GI and liver involvement at GVHD onset regardless of other organ involvement (n = 35), REG3α concentrations at the onset of liver GVHD were significantly higher than concentrations at onset of non-GVHD hyperbilirubinemia (supplemental Figure 2). Comparing concentrations from all 35 liver GVHD patients with those from the 25 patients with non-GVHD liver complications, the AUC of the REG3α ROC curve improved to 0.69, whereas curves for KRT18 and HGF performed more poorly (0.54 and 0.57, respectively), reinforcing the strength of REG3α as an LGI GVHD biomarker and lack of specificity of KRT18 and HGF as visceral GVHD biomarkers.

In conclusion, REG3α performs better than HGF and KRT18 as a diagnostic biomarker of LGI GVHD. All 3 biomarkers predicted day 28 nonresponse to therapy, and both REG3α and HGF are good prognostic markers for 1-year NRM in patients with LGI GVHD. These findings should be validated in a prospective, multicenter study. Hyperbilirubinemia was an uncommon occurrence in our patient cohort, and the preliminary findings from this study warrant further investigation. In addition, a dedicated proteomics search should be performed to identify potential biomarkers specific to liver GVHD pathophysiology. This search should then be validated in a multicenter trial because of the rarity of this post-HCT complication and to minimize any potential center effect.

Acknowledgments

This study was supported by grants from the National Institutes of Health (RC1-HL-101102, P01-CA039542, and T32-HL007622), the Hartwell Foundation, and the Doris Duke Charitable Foundation. J.L.M.F. is a clinical research professor of the American Cancer Society and a visiting fellow of the Oxford All Souls College. S.P. is an investigator of the Eric Hartwell fund and the Amy Strelzer Manasevit Research Program.

Authorship

Contribution: A.C.H. designed and planned the experiments, performed the research, performed the data collection and quality assurance, analyzed the data, and wrote the manuscript; J.L.M.F. planned the study, interpreted the data, and wrote the manuscript; T.M.B. was the study statistician and wrote the manuscript; E.H., T.T., J.E.L., S.W.C, K.L., K.A., D.R.C., and P.R. contributed to patient accrual, clinical data collection, and quality assurance, to discussions of the research, and to writing of the manuscript; M.V.L. performed the experiments and wrote the manuscript; and S.P. conceived and planned the study design, performed the experiments, interpreted the data, and wrote the manuscript.

Conflict-of-interest disclosure: The authors declare no competing financial interests.

Correspondence: Dr Sophie Paczesny, Blood and Marrow Transplant Program, University of Michigan Comprehensive Cancer Center, Room 6410, 1500 E Medical Center Dr, Ann Arbor, MI, 48109-5942; e-mail: sophiep@med.umich.edu.

References

1. Cutler C, Antin JH. Manifestation and treatment of acute graft-versus-host-disease. In: Appelbaum F, Forman SJ, Negrin RS, Blume KG, eds. *Thomas' Hematopoietic Cell Transplantation*. 4th Ed. London, United Kingdom: Blackwell Publishing; 2009:1287-1303.
2. Ferrara JL, Levine JE, Reddy P, Holler E. Graft-versus-host disease. *Lancet*. 2009;373:1550-1561.
3. Welniak LA, Blazar BR, Murphy WJ. Immunobiology of allogeneic hematopoietic stem cell transplantation. *Annu Rev Immunol*. 2007;25:139-170.
4. Ferrara JL, Harris AC, Greenson JK, et al. Regenerating islet-derived 3 alpha is a biomarker of gastrointestinal graft-versus-host disease. *Blood*. 2011;118(25):6702-6708.
5. Paczesny S, Krijanovski OI, Braun TM, et al. A biomarker panel for acute graft-versus-host disease. *Blood*. 2009;113(2):273-278.
6. Luft T, Conzelmann M, Benner A, et al. Serum cytokeratin-18 fragments as quantitative markers of epithelial apoptosis in liver and intestinal graft-versus-host disease. *Blood*. 2007;110(13):4535-4542.
7. Luft T, Dietrich S, Falk C, et al. Steroid-refractory GVHD: T-cell attack within a vulnerable endothelial system. *Blood*. 2011;118(6):1685-1692.
8. Lee KH, Choi SJ, Lee JH, et al. Prognostic factors identifiable at the time of onset of acute graft-versus-host disease after allogeneic hematopoietic cell transplantation. *Haematologica*. 2005;90(7):939-948.
9. Robin M, Porcher R, de Castro R, et al. Initial liver involvement in acute GVHD is predictive for non-relapse mortality. *Transplantation*. 2009;88(9):1131-1136.
10. Gooley TA, Chien JW, Pergam SA, et al. Reduced mortality after allogeneic hematopoietic-cell transplantation. *N Engl J Med*. 2010;363(22):2091-2101.
11. MacMillan ML, Weisdorf DJ, Wagner JE, et al. Response of 443 patients to steroids as primary therapy for acute graft-versus-host disease: comparison of grading systems. *Biol Blood Marrow Transplant*. 2002;8(7):387-394.
12. Weisdorf D, Haake R, Blazar B, et al. Treatment of moderate/severe acute graft-versus-host disease after allogeneic bone marrow transplantation: an analysis of clinical risk features and outcome. *Blood*. 1990;75(4):1024-1030.
13. Fine JP, Gray RJ. A proportional hazards model for the subdistribution of a competing risk. *J Am Stat Assoc*. 1999;94:496-509.
14. Mielcarek M, Storer BE, Boeckh M, et al. Initial therapy of acute graft-versus-host disease with low-dose prednisone does not compromise patient outcomes. *Blood*. 2009;113(13):2888-2894.
15. Chu PG, Weiss LM. Keratin expression in human tissues and neoplasms. *Histopathology*. 2002;40(5):403-439.
16. MacMillan ML, DeFor TE, Weisdorf DJ. The best endpoint for acute GVHD treatment trials. *Blood*. 2010;115(26):5412-5417.
17. Levine JE, Logan B, Wu J, et al. Graft-versus-host disease treatment: predictors of survival. *Biol Blood Marrow Transplant*. 2010;16(12):1693-1699.
18. Saliba RM, Couriel DR, Giralt S, et al. Prognostic value of response after upfront therapy for acute GVHD. *Bone Marrow Transplant*. 2012;47(1):125-131.

The EMBO Journal (2012) 31, 2994–3007 | © 2012 European Molecular Biology Organization | All Rights Reserved 0261-4189/12
www.embojournal.org

THE EMBO JOURNAL

Chd2 interacts with H3.3 to determine myogenic cell fate

Akihito Harada[1], Seiji Okada[1], Daijiro Konno[2], Jun Odawara[1], Tomohiko Yoshimi[3], Saori Yoshimura[3], Hiromi Kumamaru[1], Hirokazu Saiwai[1], Toshiaki Tsubota[4], Hitoshi Kurumizaka[5], Koichi Akashi[6], Taro Tachibana[3], Anthony N Imbalzano[7] and Yasuyuki Ohkawa[1,*]

[1]Department of Advanced Medical Initiatives, JST-CREST, Faculty of Medicine, Kyushu University, Fukuoka, Japan, [2]Laboratory for Cell Asymmetry, Center for Developmental Biology, RIKEN, Kobe, Japan, [3]Department of Bioengineering, Graduate School of Engineering, Osaka City University, Osaka, Japan, [4]Experimental Research Center for Infectious Diseases, Institute for Virus Research, Kyoto University, Kyoto, Japan, [5]Laboratory of Structural Biology, Graduate School of Advanced Science and Engineering, Waseda University, Tokyo, Japan, [6]Department of Medicine and Biosystemic Science, Faculty of Medicine, Kyushu University, Fukuoka, Japan and [7]Department of Cell Biology, University of Massachusetts Medical School, Worcester, MA, USA

Cell differentiation is mediated by lineage-determining transcription factors. We show that chromodomain helicase DNA-binding domain 2 (Chd2), a SNF2 chromatin remodelling enzyme family member, interacts with MyoD and myogenic gene regulatory sequences to specifically mark these loci via deposition of the histone variant H3.3 prior to cell differentiation. Directed and genome-wide analysis of endogenous H3.3 incorporation demonstrates that knockdown of Chd2 prevents H3.3 deposition at differentiation-dependent, but not housekeeping, genes and inhibits myogenic gene activation. The data indicate that MyoD determines cell fate and facilitates differentiation-dependent gene expression through Chd2-dependent deposition of H3.3 at myogenic loci prior to differentiation.
The EMBO Journal (2012) **31**, 2994–3007. doi:10.1038/emboj.2012.136; Published online 8 May 2012
Subject Categories: chromatin & transcription; differentiation & death
Keywords: chromatin; differentiation; histone variant; myogenesis

Introduction

The mechanisms by which a lineage-committed but undifferentiated cell maintains the ability to specifically activate the appropriate differentiation programme upon differentiation signalling is poorly understood. Activation of differentiation-specific genes depends on the binding of lineage-determining transcription factors to specific regulatory regions and on the appropriate regulation of chromatin structure. Hence, the future gene expression pattern of the differentiated cell must be present in the chromatin structure of the undifferentiated cell in the form of some sort of marking of the genome. However, how this marking is established and recognized is not clear.

To elucidate the mechanism of this marking of the whole genome, extensive study of chromatin structure in relation to cell differentiation has been undertaken. For example, methylation of specific DNA sequences by DNA methyltransferase activity is required for mouse development (Okano *et al*, 1999). It has also been reported that maintenance of histone modifications in the respective promoters of the HNF-1, HNF-4 and albumin genes through the cell cycle in hepatocytes facilitates expression of these genes (Kouskouti and Talianidis, 2005). Moreover, examination of histone acetylation levels in embryonic stem (ES) cells indicates hyperacetylation of histones H3 and H4 in the undifferentiated state (Meshorer *et al*, 2006). In fact, gene expression patterns are marked from an early stage for the maintenance of differentiation. Recently, characteristic histone variants have been identified that mark the active and the inactive state (Hake *et al*, 2006). For example, H3.3 has been found to be enriched with active H3K4me2/3, H3K9Ac and H3K14Ac marks and to be predominantly incorporated in the regulatory regions of transcriptionally active genes (Wirbelauer *et al*, 2005). In contrast, H3.2 is enriched with repressive H3K27me2/3 and H3K9me2 marks (Hake *et al*, 2006; Garcia *et al*, 2007). Therefore, exchange of histone variants is involved in the appropriate switching on and off of genes. In mouse ES cells, H3.3 is found at many developmental regulatory genes that are 'bivalent genes', marked with transcription-repressing H3K27me and transcription-activating H3K4me3 (Goldberg *et al*, 2010). In addition, over-expression of H3.3 results in maintenance of the transcriptionally active pattern of gene expression in specific tissue (Ng and Gurdon, 2008). These findings show that replacement of the histone variant (such as H3.3) contributes to the determination of selective gene expression, likely before histone modification (Hake and Allis, 2006).

Induction of transcriptional factors is also a method of controlling gene expression. For example, the myogenic transcription factor MyoD induces myogenic differentiation and can even promote reprogramming from a non-muscle cell to a muscle cell (Davis *et al*, 1987). A similar phenomenon is observed by introduction of specific lineage-determining regulators such as PPARγ2, or the four transcription factors that regulate formation of the induced pluripotent stem cell (Tontonoz *et al*, 1994; Takahashi and Yamanaka, 2006). Therefore, these transcription factors are required for reprogramming and alteration of the genomic state. It is known that these transcription factors regulate chromatin structure; to date, histone modification and chromatin remodelling have been identified as resultant changes, but a relationship between transcription factors and the type of

*Corresponding author. Department of Advanced Medical Initiatives, JST-CREST, Faculty of Medicine, Kyushu University, 3-1-1 Maidashi, Fukuoka 812-8582, Japan. Tel.: +81 92 642 6216; Fax: +81 92 642 6099; E-mail: yohkawa@epigenetics.med.kyushu-u.ac.jp

Received: 6 October 2011; accepted: 18 April 2012; published online: 8 May 2012

histone variant (such as incorporation of H3.3) has not been recorded.

MyoD is expressed in committed but undifferentiated cells, but how MyoD identifies genes for activation during differentiation is unknown. We hypothesized that a chromatin modifying or remodelling enzyme was likely involved. We identified chromodomain helicase DNA-binding domain 2 (Chd2), a member of the SNF2 family of chromatin remodelling enzymes, as a MyoD-interacting protein that facilitates cell fate determination via marking of myogenic genes by incorporation of the variant histone H3.3.

Results

Chd2 interacts with MyoD

It was previously shown that MyoD associates with Brg1, an enzyme of the mammalian SWI/SNF class of ATP-dependent chromatin remodelers, in differentiating muscle cells (Simone *et al*, 2004; de la Serna *et al*, 2005). We theorized that chromatin remodelling enzymes also might interact with MyoD in undifferentiated cells. Using monoclonal antibodies we had generated against Brg1, Brm, Chd1, and Chd2 (Ohkawa *et al*, 2009; Okada *et al*, 2009; Harada *et al*, 2010b; Yoshimura *et al*, 2010), we identified Chd2, but not Brg1 or Brm, as a MyoD co-immunoprecipitation (co-IP) product in C2C12 myoblasts (Figure 1A; Supplementary Figure S1A). The closely related protein Chd1 (60% homology) was not co-immunoprecipitated with MyoD. Reciprocal co-IP confirmed that Chd2 interacted with MyoD (Figure 1A). Additionally a proximity ligation assay (PLA) was used to demonstrate interaction between Chd2 and MyoD. Interactions between Chd2 and MyoD were observed in both myoblasts and differentiated cells (Figure 1B). As a control, we examined interactions between MyoD and Brg1, which as expected, were greatly enhanced in differentiated cells (Figure 1C). Immunocytochemistry revealed that a subset of Chd2 and MyoD, both of which are exclusively nuclear, were co-localized prior to cell differentiation (Supplementary Figure S1B). A cross-correlation analysis (vanSteensel *et al*, 1996) of confocal images of Chd2 and MyoD provided further support for co-localization in myoblasts as well as in differentiated C2C12 cells, suggesting that the MyoD–Chd2 interaction persists during differentiation (Supplementary Figure S1B). The specificity of the MyoD–Chd2 association was further assessed by examining co-localization between MyoD and Chd1. Whereas 35–40% of the MyoD co-localized with Chd2 in both myoblast and myotube nuclei, only 7–15% of the MyoD co-localized with Chd1 (Supplementary Figure S1C). Chd2 protein levels were not significantly different in myoblasts and in differentiated cells (Figure 1D).

Chd2 binds to myogenic gene promoters

Chromatin IP (ChIP) was used to analyse whether Chd2 is localized at differentiation-dependent myogenic genes. Because Chd2 was identified as a MyoD-interacting protein, we focused on regulatory sequences containing E-boxes. Chd2 interacted with the promoters of numerous myogenic gene loci in undifferentiated as well as differentiated C2C12 cells but not with housekeeping genes such as *Gapdh* or the inactive *Igh* enhancer (Figure 2A; Supplementary Figure S1D). To examine whether Chd2 recruitment was dependent on MyoD, we performed ChIP assays in NIH3T3 cells directed to undergo myogenesis by ectopic expression of MyoD (Davis *et al*, 1987). We observed MyoD-dependent binding of Chd2 specifically at myogenic gene promoters but not at housekeeping or silent gene promoters (Figure 2B). Coincident binding of MyoD at these same myogenic sequences was confirmed (Supplementary Figure S1E). Western blot analysis showed that the expression of MyoD in these cells did not alter Chd2 levels (Figure 2C). In addition, MyoD levels in these cells were not over-expressed relative to MyoD expression in C2C12 cells (Supplementary Figure S1F).

To further demonstrate that Chd2 recruitment is MyoD-dependent, we reduced the expression of MyoD in C2C12 cells by siRNA treatment and observed that Chd2 binding to myogenic genes did not occur (Figure 2D). Western blot analysis confirmed that MyoD protein levels were reduced by the siRNA treatment and that Chd2 protein levels were not

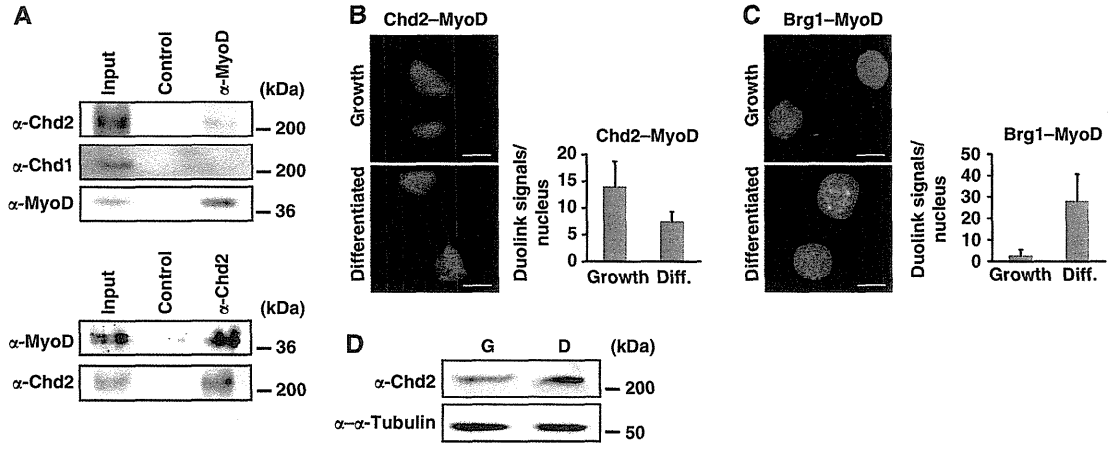

Figure 1 Chd2 interacts with MyoD. (**A**) Reciprocal IPs were performed from C2C12 myoblast extracts using MyoD- and Chd2-specific antibodies or IgG as a control. (**B**) PLAs indicating interaction of MyoD and Chd2 in both proliferating myoblasts and differentiated cells, in contrast to (**C**) the differentiation-specific interactions of MyoD and Brg1. Quantification represents the mean of three independent experiments, each of which analysed at least three separate fields ± s.d. Scale bars = 12.5 μm. (**D**) Western blot analysis of Chd2 levels in C2C12 cells under growth (G) or differentiation (D) conditions.

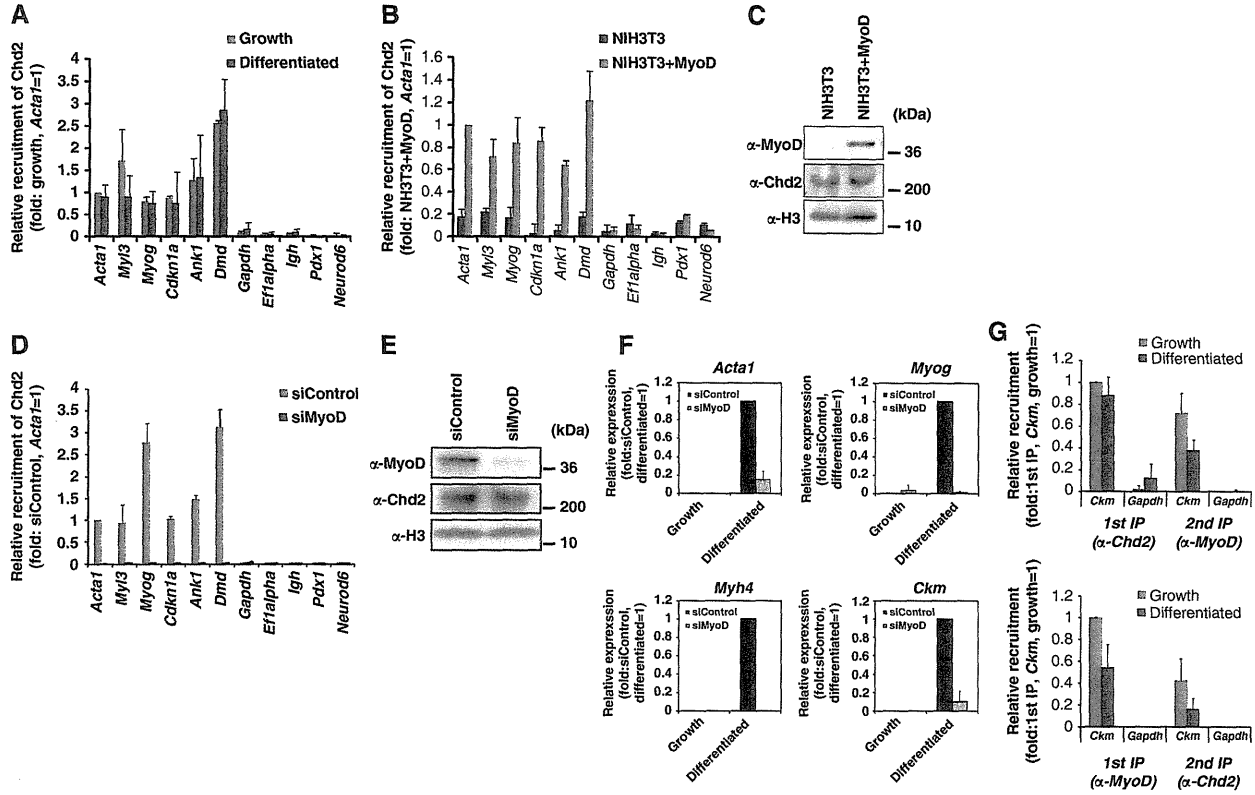

Figure 2 Chd2 interacts with MyoD and myogenic gene regulatory sequences. (**A**) ChIP assays for Chd2 binding at differentiation-dependent and skeletal muscle-specific (*Acta1, Myl3, Myog, Cdkn1a, Ank1, Dmd*), housekeeping (*Gapdh, Ef1alpha*), and silent (*IgH* enhancer, *Pdx1, Neurod6*) gene promoters were performed in C2C12 cells under growth and differentiated conditions. Relative recruitment was defined as the ratio of amplification of the PCR product relative to 1% of input genomic DNA. Values obtained from *Acta1* at the growth stage were defined as 1 and all other values were expressed relative to that value. Each value was standardized by the amplification efficiency of each primer pair. Quantification represents the mean of three independent experiments ± s.d. (**B**) Ectopic expression of MyoD induces Chd2 recruitment onto the promoter regions of myogenic genes. ChIP assays were performed as in (**A**) in fibroblast cells expressing MyoD or empty vector that were subjected to the differentiation protocol. (**C**) Western blot analysis for MyoD and Chd2 expression in MyoD-infected fibroblasts. H3 levels were monitored as a control. (**D**) siRNA-mediated MyoD knockdown inhibits Chd2 recruitment onto the promoter regions of myogenic genes. ChIP assays for Chd2 binding were performed as described in (**A**) in C2C12 myoblasts treated with either control siRNA or MyoD siRNA. (**E**) siRNA-mediated knockdown of the endogenous MyoD protein in C2C12 cells. A western blot analysis of C2C12 cells treated with either control siRNA or MyoD siRNA using antibodies against MyoD, Chd2, and H3 is shown. (**F**) Relative expression of skeletal muscle marker genes was reduced in C2C12 cells treated with MyoD siRNA. The levels of the indicated mRNAs were analysed by Q-PCR. The values in the differentiated cells expressing control siRNA were set to 1. Data represent the average of three independent experiments ± s.d. (**G**) Chd2 and MyoD co-recruitment at the *Ckm* but not the *Gapdh* promoter is shown by re-ChIP. Re-ChIP experiments sequentially used antibodies against Chd2 and MyoD, as indicated. Relative recruitment was defined as the ratio of amplification of the PCR product relative to 1% of input genomic DNA. Values obtained from *Ckm* at the growth stage with 1st IP were defined as 1 and all other values were expressed relative to that value. Each value was standardized by the amplification efficiency of each primer pair. Quantification represents the mean of three independent experiments ± s.d.

affected (Figure 2E). As expected, siRNA-mediated reduction of MyoD also compromised differentiation-dependent myogenic gene activation (Figure 2F). We then performed re-ChIP assays (Ohkawa *et al*, 2006). In C2C12 myoblasts maintained in growth media, Chd2 was simultaneously present with MyoD on the *Ckm* promoter but not on the *Gapdh* locus (Figure 2G). In differentiated C2C12 cells, Chd2 and MyoD were both present at the *Ckm* locus, but to a somewhat lesser extent than in myoblasts (Figure 2G). Collectively, these data strongly suggest that Chd2 is targeted to the *Ckm* promoter via MyoD and are consistent with results demonstrating widespread MyoD binding to myogenic genes in undifferentiated myoblasts (Cao *et al*, 2010).

Chd2 promotes myogenic gene expression

To explore the requirement for Chd2 in myogenesis, we suppressed Chd2 expression by stably introducing two microRNAs (miRNA) that target *Chd2* ($Chd2^{miR3139}$ and $Chd2^{miR5111}$) in C2C12 cells. We used cells stably transfected with *lacZ*-targeted miRNA ($Chd2^{WT}$) as a control. To indirectly monitor miRNA expression, enhanced green fluorescent protein—nuclear localization signal (EGFP–NLS) was expressed co-cistronically with the miRNA (Figure 3A). Analysis of myogenic gene expression in these cells indicated that myosin heavy chain expression, which is a late myogenic marker, was completely suppressed in both $Chd2^{miR3139}$ and $Chd2^{miR5111}$-expressing cells ($n=70$ and 63 GFP-positive cells, respectively; Figure 3A). The expression of myogenin, which is a marker of the early phase of myogenesis, was decreased in both cell lines to 6% ($Chd2^{miR3139}$, $n=109$ GFP-positive cells) and 13% of wild-type (WT) ($Chd2^{miR5111}$, $n=76$ GFP-positive cells; Figure 3A). Moreover, myotube formation was not observed in either miRNA-expressing cell line upon differentiation. Compared with controls, the mRNA

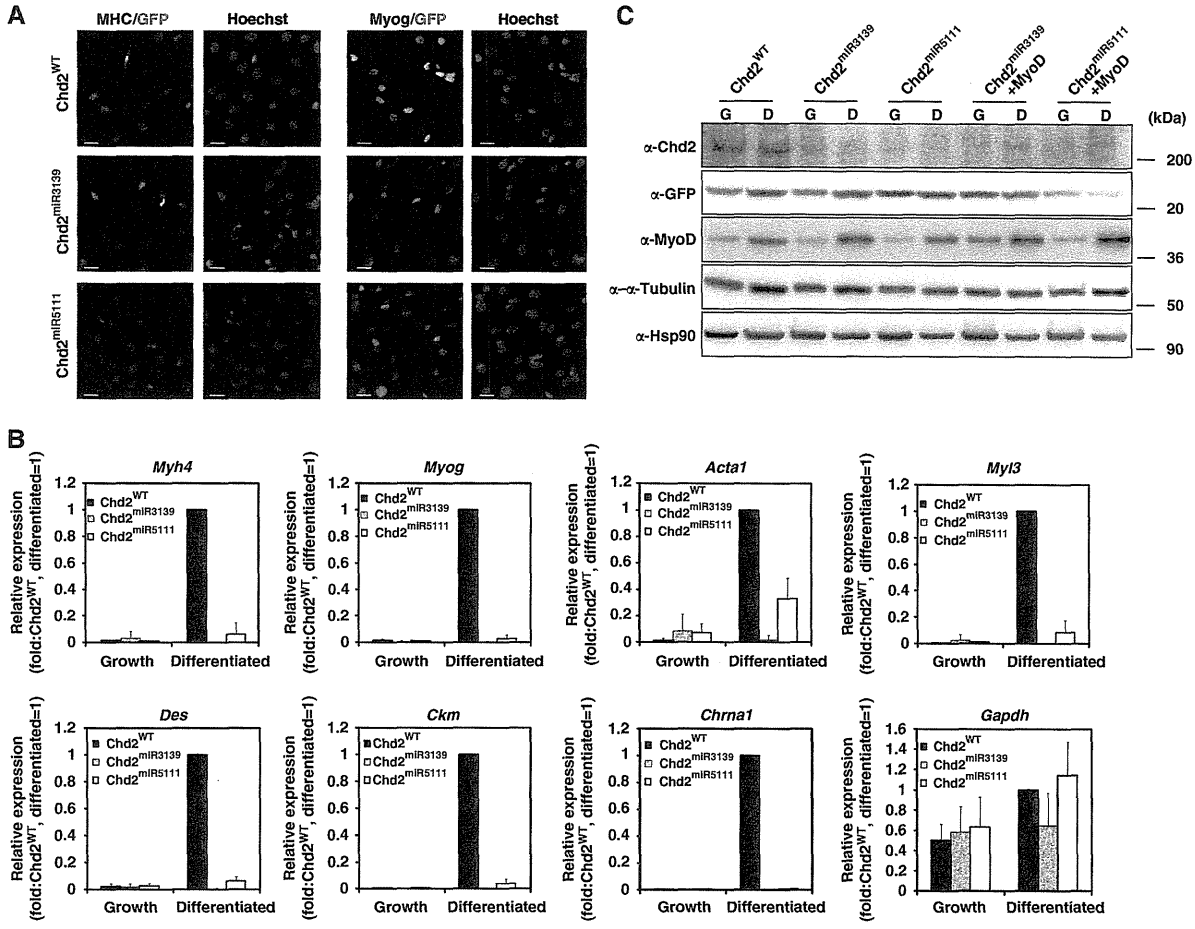

Figure 3 Chd2 is required for skeletal muscle differentiation. (**A**) The expression of myogenin (Myog) and myosin heavy chain (MHC) was not induced in C2C12 cells when Chd2 expression was suppressed by miRNAs targeting *Chd2*. To indirectly monitor miRNA expression, EGFP–NLS (EGFP fused with a nuclear transport signal) was expressed co-cistronically with miRNA. Scale bars = 5 μm. (**B**) The transcription of skeletal muscle marker genes was suppressed in C2C12 cells expressing miRNA targeting Chd2. mRNA levels were analysed by Q-PCR; data represent the average of three independent experiments ± s.d. *Gapdh* levels are shown as a control. (**C**) Western blot evaluating Chd2 protein knockdown and the expression of MyoD and other indicated proteins.

expression levels of every differentiation-dependent myogenic gene tested was significantly repressed in $Chd2^{miR3139}$ and $Chd2^{miR5111}$-expressing cells (Figure 3B). In contrast, expression of the housekeeping gene, *Gapdh*, was unaffected (Figure 3B).

Control experiments determined that *Chd2* transcript levels were not affected in cells expressing the Chd2-targeting miRNAs (Supplementary Figure S2A), but Chd2 protein expression was repressed (Figure 3C). This suggests that the specific miRNAs functioned as translational repressors of Chd2. The GFP expression level remained consistent, suggesting no significant differences in miRNA expression between the cells (Figure 3C). In addition, no significant differences in the expression of MyoD were observed between $Chd2^{WT}$ and miRNA-expressing cells, indicating that Chd2 was not regulating the expression of MyoD (Figure 3C). To confirm that changes in MyoD levels observed during differentiation did not alter Chd2 expression, we ectopically expressed MyoD in the Chd2 miRNA-expressing cells and showed that Chd2 expression (Figure 3C) and differentiation-dependent gene expression (Supplementary Figure S2B) were not rescued. We also determined that cell-cycle progression was not affected by miRNA expression in undifferentiated or differentiated cells as measured by FACS analysis (Supplementary Figure S2C) and western blot analysis of cyclins A and E (Supplementary Figure S2D). These data indicate that Chd2 is not indirectly affecting myogenic gene expression via alteration of cell-cycle arrest.

To complement these studies showing a requirement for Chd2 in myogenic differentiation, we reduced Chd2 expression by introducing siRNA molecules that target Chd2. siRNA-treated cells did not form myotubes as demonstrated by MHC staining (Supplementary Figure S3A) and were compromised for differentiation-specific gene expression (Supplementary Figure S3B). Western analysis demonstrated the reduction in Chd2 levels in siRNA-treated cells and no effect on MyoD levels (Supplementary Figure S3C).

To further confirm a Chd2-specific function in myogenic gene induction, we rescued the inhibition of *Chd2* expression by miRNA via the exogenous introduction of competitive mRNA fragments (*Chd2*-3011-3283 or *Chd2*-5004-5177) that were linked to the monomeric Kusabira Orange (mKO1) fluorescent protein containing a nuclear localization signal (Karasawa *et al*, 2004). In differentiated cells expressing

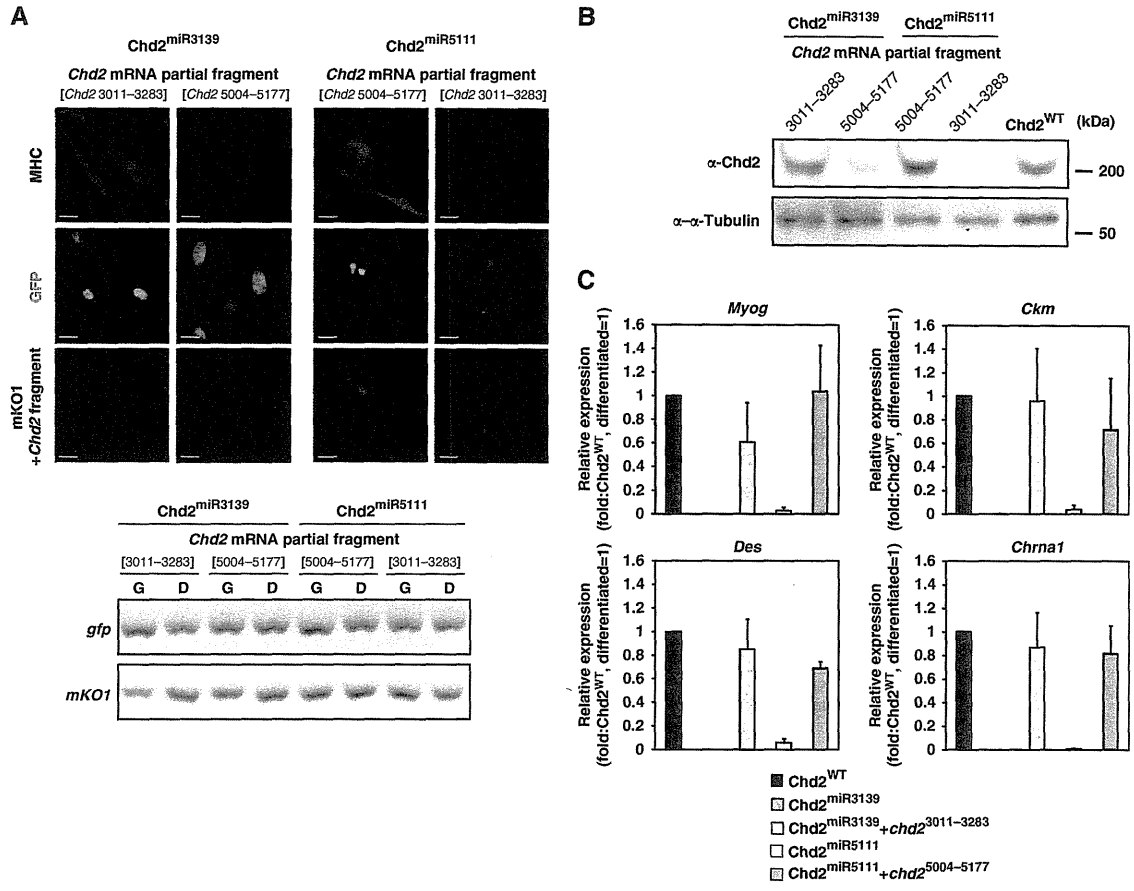

Figure 4 Myogenic phenotype is rescued by a forced expression of *Chd2* partial mRNA in Chd2 knockdown cells. (**A**) The expression of myosin heavy chain (MHC; blue) was re-induced in C2C12 cells expressing miRNAs targeting *Chd2* and a *Chd2* partial mRNA that competes each miRNA. To indirectly monitor miRNA and *Chd2* partial mRNA expression, EGFP–NLS (EGFP fused with a nuclear transport signal) and mKO1–NLS (mKO1 fused with a nuclear transport signal) were expressed co-cistronically with the miRNA and *Chd2* partial mRNA, respectively. Scale bars = 5 μm. Q-PCR analysis confirms equivalent expression of GFP and mKO1 in each sample (lower panel). (**B**) Chd2 expression was rescued in C2C12 cells expressing miRNAs targeting *Chd2* and the competing *Chd2* partial mRNA. Western blot analysis utilized antibodies against Chd2 and α-tubulin. (**C**) The transcription of skeletal muscle marker genes was rescued in C2C12 cells expressing miRNAs targeting *Chd2* and the competing *Chd2* partial mRNA. The levels of the indicated mRNAs were analysed by Q-PCR; data represent the average of three independent experiments ± s.d.

Chd2^{miR3139}, introduction of a competitive mRNA (*Chd2*-3011-3283) but not an mRNA from a different region of *Chd2* (*Chd2*-5004-5177), restored MHC expression (Figure 4A). Similarly, introduction of the mRNA (*Chd2*-5004-5177) rescued MHC expression in Chd2^{miR5111}-treated cells whereas introduction of the (*Chd2*-3011-3283) mRNA did not (Figure 4A). mKO1 expression levels were monitored to confirm equal expression of the competitive mRNAs in the cells (Figure 4A). Furthermore, under conditions where MHC expression was restored, we observed restoration of Chd2 protein levels (Figure 4B) and expression of *Myog*, *Ckm*, *Des*, and *Chrna1* at levels comparable to WT (Figure 4C).

As a complement to this set of experiments, we attempted to rescue the miRNA-mediated inhibition of *Chd2* expression and the inhibition of myogenesis via the exogenous introduction of full-length Chd2 cDNA or a Chd2 deletion mutant (Chd2-chromodomain deletion Δ-281–512 aa). Chromodomains facilitate interaction of proteins with chromatin via interaction with methylated histones (Pray-Grant *et al*, 2005). The constructs utilized were Flag-tagged and co-expressed the monomeric Kusabira Orange 2 (mKO2) fluorescent protein (Karasawa *et al*, 2004; Sakaue-Sawano *et al*, 2008). In differentiated cells expressing either Chd2^{miR3139} or Chd2^{miR5111}, introduction of full-length Chd2 restored MHC expression and myotube formation, whereas expression of the Chd2 mutant lacking the chromodomain did not (Supplementary Figure S4A). Similarly, introduction of the full-length, but not the mutant Chd2, restored expression of *Acta1*, *Myog*, *Ckm*, and *Myh4* to levels comparable to those expressed in the control cells (Supplementary Figure S4B). Under conditions where myogenic gene expression and differentiation were restored, we observed restoration of Chd2 protein levels (Supplementary Figure S4C).

Chd2 interacts with histone H3.3

Since we observed that Chd2 was present at differentiation-dependent genes in proliferating myoblasts, we wished to address whether Chd2 might facilitate myogenic gene activation prior to the onset of differentiation and myogenic gene expression. CHD1, a related member of the CHD family, incorporates H3.3 into the nucleosome (Konev *et al*, 2007). H3.3 is a variant of H3 that is incorporated at

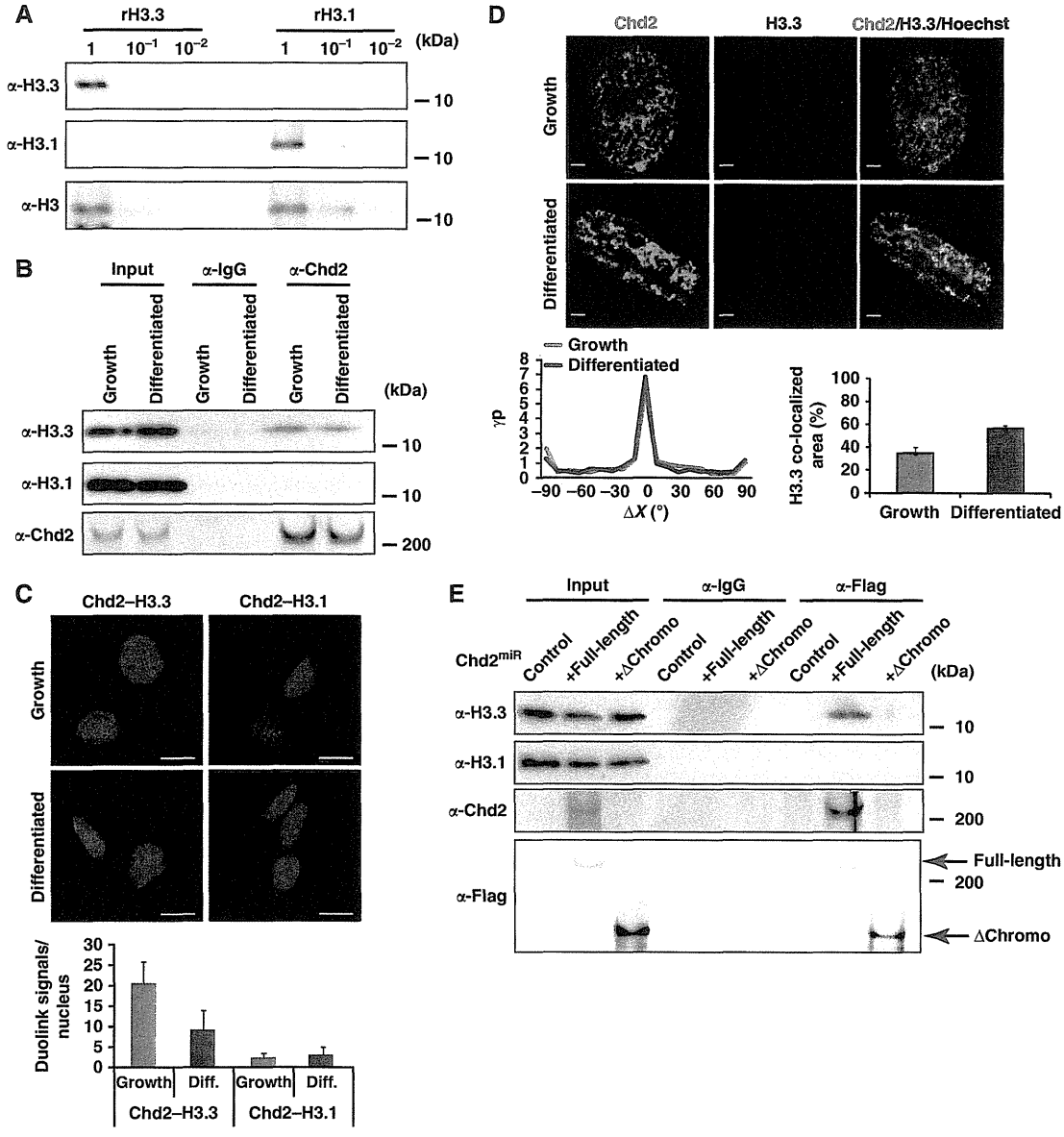

Figure 5 Chd2 interacts with H3.3 prior to and during skeletal muscle differentiation. (**A**) H3.3 antibody specifically discriminates between H3.3 and H3.1. Serial dilutions of purified recombinant H3.1 and H3.3 protein were evaluated by immunoblotting using the H3.3 and H3.1 monoclonal antibodies and the H3 polyclonal antibody. Detection of H3.3, H3.1, and H3 was performed on the same membrane. (**B**) IP from C2C12 cells using control IgG or Chd2-specific antibodies shows an interaction between Chd2 and H3.3. (**C**) PLAs indicating the frequency of interaction between H3.3 and Chd2 and between H3.1 and Chd2 in both proliferating myoblasts and differentiated cells. Quantification represents the mean of three independent experiments, each of which analysed at least three separate fields ± s.d. Scale bars = 12.5 μm. (**D**) C2C12 cells at growth and differentiated stages were immunostained with antibodies to Chd2 (green) and H3.3 (red) to show Chd2 and H3.3 co-localization. Confocal images, cross-correlation analysis, and the amount of H3.3 interacting with Chd2 are shown. Scale bars = 1 μm. (**E**) Co-immunoprecipitation from Chd2^{miR3139} cells expressing full-length Chd2–Flag or Chd2 deletion mutant (ΔChromodomain (281–512 aa)–Flag) using control IgG or Flag-antibodies shows an interaction between full-length Chd2 and H3.3.

transcriptionally activated genes (Ahmad and Henikoff, 2002; Jin *et al*, 2009). To evaluate whether Chd2 interacts with endogenous H3.3, we generated monoclonal antibodies to specifically distinguish H3.3 from H3.1, the major H3 isoform. H3.3 differs from H3.1 at only five residues, only one of which is in the N-terminal tail (position 31). Peptides spanning amino acids 21–39 were used as antigen. The specificity of each antibody was demonstrated by specific recognition of the appropriate recombinant H3.3 or H3.1 protein (Figure 5A). Specificity of the H3.3 antibody was further demonstrated by its specific recognition of modified and unmodified H3.3 and H3.1 peptides (Supplementary Figure S5A). Epitope mapping with recombinant H3.3 and H3.1 proteins revealed that the H3.3 antibody specifically recognized the unique S31 residue present in H3.3 (Supplementary Figure S5B). Since H3.3 is primarily associated with active transcription, we performed immunostaining to gauge the extent to which the H3.3 antibody recognizes euchromatin and heterochromatin, which is marked by intense Hoechst staining. The data indicate that the H3.3

antibody primarily recognizes euchromatic regions of the genome (Supplementary Figure S5C). This result is consistent with previous work showing that exogenous H3.3 is predominantly incorporated into active gene loci (Ahmad and Henikoff, 2002; Jin *et al*, 2009). Previously, H3.3 has been found to be enriched with active H3K4me2/3 marks, but not H3K9me2 marks (Wirbelauer *et al*, 2005; Hake *et al*, 2006; Garcia *et al*, 2007). Use of the H3.3 antibody in co-localization analyses with either H3K4me3 or H3K9me3 demonstrated significant co-localization with H3K4me3 but not H3K9me3 (Supplementary Figure S5D). Collectively, the data indicate that the H3.3 antibody specifically recognizes endogenous H3.3. We also determined that neither the overall nor the chromatin-associated levels of H3.3 changed as a function of C2C12 cell differentiation (Supplementary Figure S5E). Subsequent experiments showed that Chd2 could co-immunoprecipitate with H3.3, but not H3.1, in undifferentiated cells (Figure 5B). PLA assays also indicated Chd2–H3.3 interactions in myoblasts as well as differentiated cells, whereas the frequency of Chd2–H3.1 interactions was much lower (Figure 5C). Immuno-localization studies indicated Chd2–H3.3 co-localization in both undifferentiated and differentiated cells (Figure 5D). We further analysed the Chd2 and H3.3 interaction by co-IP using $Chd2^{mir3139}$ cells that exogenously express either Flag-tagged full-length Chd2 or the chromodomain deleted Chd2 mutant. Flag-tagged full-length Chd2 was immunoprecipitated with endogenous H3.3, while the Chd2 mutant was not (Figure 5E). Collectively, these studies suggest a possible link between Chd2 function and H3.3.

Chd2 mediates H3.3 incorporation into the regulatory regions of myogenic genes prior to the onset of myogenic gene expression

ChIP assays showed that H3.3 was incorporated at both myogenic and housekeeping gene regulatory sequences, including *Gapdh*, and *Ef1alpha*, but not at silent gene loci such as *Igh*, *Pdx1*, or *Neurod6* both in myoblasts and in differentiated cells (Figure 6A). This indicates that H3.3 marks myogenic genes prior to their expression. To confirm that H3.3 in fact was incorporated prior to the expression of these genes, duplicate plates were harvested for RNA. Q-PCR evaluation of myogenic gene expression demonstrated that the myoblast samples that showed H3.3 incorporation into myogenic gene promoters were not expressing myogenic genes (Supplementary Figure S6).

We next demonstrated that H3.3 is incorporated into the regulatory regions of myogenic genes in a Chd2-dependent manner. Relative incorporation of H3.3 in $Chd2^{miR}$ ($Chd2^{miR3139}$) expressing cells was decreased in the promoter regions of each of the myogenic genes in the undifferentiated state, but Chd2 knockdown had no effect on H3.3 incorporation at the *Gapdh* and *Ef1alpha* promoters (Figure 6B). H3.3 protein levels were the same in control and in miRNA-expressing cells before and after differentiation (Figure 6C). Therefore, H3.3 expression is regulated in a Chd2-independent manner. We further evaluated whether H3.3 incorporation into myogenic gene loci was MyoD-dependent. Introduction of MyoD into fibroblast cells preferentially induced H3.3 incorporation at myogenic genes without affecting H3.3 incorporation at housekeeping or silent gene loci (Figure 6D). Similarly, knockdown of MyoD in C2C12 myoblasts prevented H3.3 incorporation at myogenic, but not housekeeping genes (Figure 6E). In summary, H3.3 incorporation at myogenic genes occurs prior to differentiation and prior to myogenic gene expression in a Chd2- and MyoD-dependent manner.

Genome-wide analysis of H3.3 incorporation has been performed in HeLa and in ES cells using epitope-tagged H3.3 (Jin *et al*, 2009; Goldberg *et al*, 2010). We attempted ChIP-seq using the H3.3 antibody to evaluate the distribution of endogenous H3.3 and the Chd2 dependency of H3.3 deposition over the whole myoblast genome. First, the regions where H3.3 was incorporated in each chromosome were analysed by Boxplot. Total incorporation of H3.3 was almost equal in each chromosome in $Chd2^{WT}$ cells, with an average of about 0.63% (Figure 7A), showing that endogenous H3.3 is incorporated into a limited region of the genome. In contrast, the percentage of H3.3-incorporating regions in $Chd2^{miR3139}$ cells was decreased to about 0.27%. The fact that incorporation of H3.3 was not completely eliminated likely reflects the fact that H3.3 is also incorporated into the genome by other factors such as Hira and Chd1 (Ray-Gallet *et al*, 2002; Konev *et al*, 2007). The entire length of every annotated gene was defined as 1 and the levels of H3.3 incorporation at all gene loci were plotted (Supplementary Figure S7A). The results showed H3.3 incorporation at the transcription start sites (TSS), the transcription end sites (TES) and throughout the gene body. Interestingly, Chd2 reduction affected the incorporation of H3.3 at the TSS at a genome-wide level (Supplementary Figure S7A). These data differ from previous reports where H3.3 was localized immediately upstream of the TSS in HeLa cells (Jin *et al*, 2009; Goldberg *et al*, 2010) and was depleted from the TSS in ES cells (Jin *et al*, 2009; Goldberg *et al*, 2010), suggesting that H3.3 deposition in the vicinity of TSS may be cell-type specific.

To evaluate whether the genome marking derived from incorporation of H3.3 by Chd2 occurred at differentiation-specific genes, we analysed incorporation of H3.3 into the TSS relative to sequences immediately upstream and downstream at genes that were reported to be upregulated during C2C12 differentiation (Tomczak *et al*, 2004) (Supplementary Dataset 1). Analysis of H3.3 incorporation at differentiation-induced genes in $Chd2^{WT}$ cells indicated that H3.3 is significantly enriched around the TSS of the skeletal muscle-specific genes ($n = 545$) compared with enrichment in $Chd2^{miR}$-expressing cells (Figure 7B). In cells expressing Chd2-targeting miRNAs, we noted that a significant percentage of the genes showed no H3.3 incorporation while others showed reduced levels. A small percentage of genes showed redistribution of H3.3 (Figure 7B) within the locus, suggesting that Chd2 is required for deposition of H3.3 at the appropriate regions of myogenic gene loci.

Comparison of myogenic, housekeeping, and silent (Supplementary Dataset 1) genes showed that H3.3 incorporation at myogenic genes was dependent on Chd2 in the TSS region whereas incorporation at housekeeping genes was modestly affected by Chd2 knockdown (Figure 7C). Housekeeping genes were defined as those that are highly expressed in C2C12 cells 2 days before and 10 days after differentiation and were also expressed in NIH3T3 cells as previously reported (Berenjeno *et al*, 2007). Silent genes were defined as the genes that were only expressed in RAW264.7

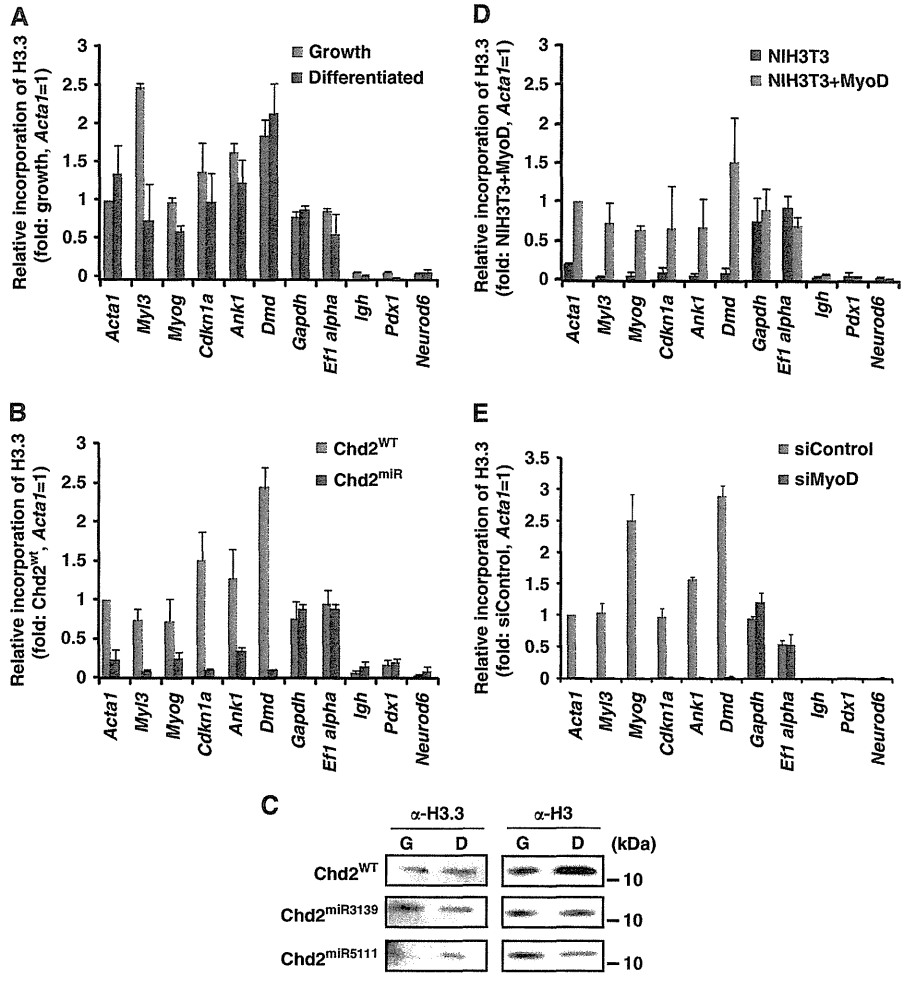

Figure 6 H3.3 incorporation at myogenic promoters occurs prior to differentiation and myogenic gene expression and is dependent on Chd2. (**A**) H3.3 incorporation at differentiation-specific myogenic gene promoters occurred prior to C2C12 cell differentiation. ChIP assays for myogenic, housekeeping, and silent genes were performed as described in Figure 2A. (**B**) Incorporation of H3.3 into myogenic gene loci is Chd2-dependent while incorporation housekeeping genes is Chd2-independent. ChIP assays for myogenic, housekeeping, and silent genes were in $Chd2^{WT}$ and $Chd2^{miR}$ ($Chd2^{miR3139}$) expressing C2C12 cells under growth conditions as described in Figure 2A. (**C**) $Chd2^{WT}$, $Chd2^{miR3139}$, and $Chd2^{miR5111}$-expressing C2C12 cells were cultured in growth medium for 1 day (G) and then shifted to differentiation medium for 48 h (**D**). H3.3 and total H3 expression levels were analysed by immunoblotting. (**D**) Ectopic expression of MyoD induces H3.3 incorporation at the promoter regions of myogenic genes. ChIP assays were performed as in Figure 2 in fibroblast cells expressing MyoD or empty vector. (**E**) siRNA-mediated MyoD knockdown inhibits H3.3 recruitment onto the promoter regions of myogenic, but not housekeeping, genes. ChIP assays were performed as in Figure 2 in C2C12 cells treated with either control siRNA or MyoD siRNA.

cells as previously reported (Covert *et al*, 2009) but not in C2C12 cells or in NIH3T3 cells. Silent genes were devoid of H3.3, but reduction of Chd2 levels caused a small number of genes to incorporate H3.3 around the TSS (Figure 7C). We then examined sequences at the transcriptional end sites (TES) region, which demonstrated that H3.3 incorporation at myogenic genes was enriched at the TES in a Chd2-dependent manner (Figure 7D). For reasons that are not understood, reduction of Chd2 levels increased H3.3 incorporation at sequences upstream of housekeeping gene TES but not at the TES itself, whereas silent genes were devoid of H3.3 at the TES (Figure 7D). We confirmed enrichment of H3.3 at the TSS and TES of the same set of myogenic genes in a different cell culture model for myogenesis. Exogenous expression of MyoD in NIH3T3 fibroblasts selectively induced H3.3 incorporation at the TSS and TES regions of muscle-specific genes relative to incorporation of H3.3 at these genes in mock-treated fibroblasts (Figure 7E). This result also demonstrates the MyoD dependency of H3.3 incorporation at myogenic loci. Finally, because the data indicated that Chd2 are incorporated at myogenic genes prior to differentiation and gene expression, we directly compared H3.3 incorporation across muscle-specific, housekeeping, and silent genes in undifferentiated and differentiated C2C12 cells to determine whether H3.3 incorporation was altered by differentiation and the activation of myogenic gene expression. At myogenic loci, H3.3 incorporation increased at the TSS and in the gene body upon differentiation, but minimally at the TES (Supplementary Figure S7B). Silent genes showed no H3.3 incorporation upon differentiation, and housekeeping genes showed an increase at the TSS (Supplementary Figure S7C and D). These data indicate that despite the incorporation of H3.3 across myogenic loci in undifferentiated cells, H3.3 incorporation was further increased upon differentiation and the activation of myogenic gene expression.